

Surface Science

Room 120 - Session SS+AMS-MoM

Dynamics and Mechanisms in Heterogeneous Catalysis

Moderators: Prabhakar Kasala, Brookhaven National Laboratory, Arthur Utz, Tufts University

8:15am **SS+AMS-MoM-1 Accurate Dynamical Modelling of Vibrationally Enhanced N₂ Dissociation on Ru(0001) – Implications (Not Only) for Plasma Catalysis**, *F. van den Bosch, N. Gerrits, Jörg Meyer*, Leiden University, Netherlands

INVITED

Pioneering work of Mehta et al. [1] has quantified the efficiency of plasma-enhanced over conventional (temperature-driven) heterogeneous catalysis - nurturing hopes for a future more sustainable alternative that can be easily upscaled. The focus has been on ammonia synthesis and vibrationally excited states available in the plasma, because the dissociative chemisorption of N₂ molecules on a metal catalyst is usually the rate-limiting step. Prevalent micro-kinetic modeling based on transition state theory (TST) for the reaction rates needs to be extended by introducing vibrational-state-dependent rate constants. To do so, Mehta et al. have postulated that the computationally convenient Fridman-Macheret model often used for reactions in the gas phase [2] also works for surface reactions.

Using N₂ on Ru(0001) as a representative showcase, we scrutinize the effect of vibrational excitations of N₂ on its surface reactivity by using explicit molecular dynamics on an accurate potential energy surface using the quasi-classical trajectory method [3,4]. We compute the dissociative chemisorption probabilities as a function of the initial vibrational state ranging from 0 to 10 vibrational quanta. These calculations yield vibrational efficacies of about 1.8, i.e., vibrational excitations are more considerably more effective for promoting dissociative chemisorption reactions than equivalent amounts of translation energy. We compare our findings to TST-based models and carefully analyze why they cannot capture the vibrationally enhanced dissociation correctly. Finally, we discuss these findings in the context of thermal and plasma-enabled catalysis by critically investigating which molecules dominate the reactivity.

1. P. Mehta, P. Barboun, F. A. Herrera, J. Kim, P. Rumbach, D. B. Go, J. C. Hicks, and W. F. Schneider, Overcoming Ammonia Synthesis Scaling Relations with Plasma-Enabled Catalysis, *Nat. Catal.* 1, 269 (2018). DOI: 10.1038/s41929-018-0045-1
2. A. Fridman, *Plasma Chemistry*, Cambridge University Press, Cambridge, 2008.
3. K. Shakouri, J. Behler, J. Meyer, and G.-J. Kroes, Accurate Neural Network Description of Surface Phonons in Reactive Gas-Surface Dynamics: N₂ + Ru(0001), *J. Phys. Chem. Lett.* 8, 2131 (2017). DOI: 10.1021/acs.jpcllett.7b00784
4. P. Spiering, K. Shakouri, J. Behler, G.-J. Kroes, and J. Meyer, Orbital-Dependent Electronic Friction Significantly Affects the Description of Reactive Scattering of N₂ from Ru(0001), *J. Phys. Chem. Lett.* 10, 2957 (2019). DOI: 10.1021/acs.jpcllett.9b00523

8:45am **SS+AMS-MoM-3 SSD Morton S. Traum Award Finalist Talk: A Priori Designed NiAg Single-Atom Alloys for Selective Epoxidation Reactions**, *Elizabeth E. HappeI¹*, Tufts University; *A. Jalil*, University of California at Santa Barbara; *S. Stratton*, Tulane University; *L. Cramer*, Tufts University; *P. Christopher*, University of California at Santa Barbara; *M. Montemore*, Tulane University; *E. Sykes*, Tufts University

Ethylene oxide, produced via the partial oxidation of ethylene, is among the largest volume chemicals produced by the chemical industry and has one of the largest carbon footprints. Using Ag catalysts, the reaction can achieve high selectivity ~90%, but only with a combination of promoters including Cl, Cs, and Re, and must be run at low conversions (< 15%) to avoid the total combustion of ethylene to carbon dioxide. Herein, we report a theory guided investigation demonstrating that the addition of low concentrations of Ni to Ag(111) lowers the barrier for O₂ dissociation and enables spillover of oxygen atoms to sites on the Ag surface. Temperature programmed desorption experiments quantify the facile dissociation, spillover and desorption of O₂ from NiAg(111) and demonstrate that, unlike all previous studies, Ni addition enables the population of the Ag(111) surface with atomic oxygen in near UHV pressure without having to atomize oxygen or introduce species like NO₂ or O₃. Furthermore, ambient pressure X-ray

photoelectron spectroscopy reveals that Ni not only aids in activation and spillover, but also stabilizes nucleophilic oxygen which is thought to be selective towards total oxidation. These results informed the synthesis and testing of supported catalysts which demonstrated that NiAg single-atom alloy nanoparticles produce ethylene oxide both with greater selectivity and conversion than Ag without the need for a co-flow of Cl and other promoters.

9:00am **SS+AMS-MoM-4 Effect of Surface Diffusion of Methoxy Intermediates on Methanol Decomposition on Pt/TiO₂(110)**, *C. Liu, B. Lu*, Hokkaido University, Japan; *H. Ariga-Miwa*, The University of Electro-Communications (UEC-Tokyo), Japan; *S. Ogura*, Tokyo Denki University, Japan; *K. Fukutani*, The University of Tokyo, Japan; *M. Gao, J. Hasegawa, K. Shimizu*, Hokkaido University, Japan; *K. Asakura*, Ritsumeikan University, Japan; *Satoru Takakusagi*, Hokkaido University, Japan

In oxide-supported metal catalysts, atomic-level understanding of dynamic behavior of intermediate adsorbates such as diffusion, spillover, and reverse spillover is crucial to unravel the origins of catalytic activity and product selectivity. Our previous *in situ* STM study on methanol adsorption process on a Pt/TiO₂(110) surface revealed that methoxy intermediates were formed on five-fold coordinated Ti⁴⁺ (Ti_{5c}) sites by dissociative adsorption of methanol on the Pt nanoparticles, followed by spillover to the TiO₂(110) substrate.^[1] They were mobile at room temperature. In this study, diffusion and thermal decomposition of the methoxy intermediates were examined by STM, density functional theory (DFT) calculation and temperature programmed desorption (TPD), in order to reveal how their diffusion affect activity and product selectivity in the methoxy decomposition on the Pt/TiO₂(110) surface.^[2] The TPD measurements showed that the methoxy intermediates were thermally decomposed at >350 K on the Pt sites to produce CO (dehydrogenation) and CH₄ (C-O bond scission) through their reverse spillover. We have found that activity and product selectivity for the methoxy decomposition was much dependent on the particle density, suggesting that it was controlled by diffusion of the methoxy intermediates. Decrease of the Pt nanoparticle density significantly enhanced the selectivity to CH₄, and thus we propose that Pt-TiO₂ interfacial sites are active for CH₄ formation while the other Pt sites for CO formation.

[1] S. Takakusagi, K. Fukui, R. Tero, K. Asakura, Y. Iwasawa, *Langmuir* 2010, 26, 16392.

[2] C. Liu, B. Lu, H. Ariga-Miwa, S. Ogura, T. Ozawa, K. Fukutani, M. Gao, J. Hasegawa, K. Shimizu, K. Asakura, S. Takakusagi, *J. Am. Chem. Soc.* 2023, 145, 19953.

9:15am **SS+AMS-MoM-5 Simultaneous Tracking of Ultrafast Surface and Gas-Phase Dynamics in Solid-Gas Interfacial Reactions**, *Keith Blackman, E. Segrest, G. Turner, K. Machamer, A. Gupta, M. Pathan*, University of Central Florida, Department of Physics; *N. Berriel*, University of Central Florida, Department of Material Science and Engineering; *P. Banerjee*, University of Central Florida, Department of Material Science and Engineering, Renewable Energy and Chemical Transformations Cluster (REACT); *M. Vaida*, University of Central Florida, Department of Physics, Renewable Energy and Chemical Transformations Cluster (REACT)

ABSTRACT

Real-time detection of intermediate species and final products at the surface and near-surface in interfacial solid-gas reactions is critical for an accurate understanding of heterogeneous reaction mechanisms. In this contribution, an experimental method that can simultaneously monitor the ultrafast dynamics at the surface and above the surface in photoinduced heterogeneous reactions is presented. The method relies on a combination of mass spectrometry and femtosecond pump-probe spectroscopy. As a model system, the photoinduced reaction of methyl iodide on and above a cerium oxide surface is investigated. The species that are simultaneously detected from the surface and gas-phase present distinct features in the mass spectra, such as a sharp peak followed by an adjacent broad shoulder. The sharp peak is attributed to the species detected from the surface while the broad shoulder is due to the detection of gas-phase species above the surface, as confirmed by multiple experiments. By monitoring the evolution of the sharp peak and broad shoulder as a function of the pump-probe time delay, transient signals are obtained that describe the ultrafast photoinduced reaction dynamics of methyl iodide on the surface and in gas-phase. Finally, SimION simulations are performed to confirm the origin of the ions produced on the surface and gas-phase.

¹ SSD Morton S. Traum Award Finalist

Monday Morning, November 4, 2024

9:30am **SS+AMS-MoM-6 In situ Photoemission of Ru(0001) Model Catalyst in Plasma-activated N₂-H₂ Mixtures, Roland Bliem**, Advanced Research Center for Nanolithography, Netherlands

In plasma-assisted catalysis, reactants are activated by a plasma discharge, resulting in vibrational excitation and the production of radicals and ions. Plasma catalysis with low-energy excitations has been reported to allow for remarkable efficiencies, under specific conditions even beyond the limits of thermal catalysis. More generally, the activation of strong molecular bonds in a plasma can soften the requirements on the operating conditions for important reactions, such as ammonia synthesis, and contribute options for their electrification and operation at small scales. While plasma-activation can facilitate certain reaction steps, the reaction pathway and product selectivity is still largely defined by the catalyst surface, making it key to catalyst design. However, at present the active state of catalyst surfaces in plasma is unknown, and *in situ* information on surfaces exposed to plasma is fully lacking.

Here, we follow the surface composition and chemistry of the Ru, one of the most active elements for conventional ammonia synthesis, *in situ* during exposure to plasma-activated N₂-H₂ mixtures using near-ambient pressure X-ray photoelectron spectroscopy (NAP-XPS). The activation of N₂ by a microwave discharge source results in extremely efficient sticking of nitrogen species to Ru(0001) and polycrystalline Ru surfaces, where they form nitrogen-metal bonds. The temperature-dependent stability of nitrogen species indicates the presence of at least two different configurations. The comparison of XPS spectra of plasma-exposed Ru to Ru nitride films grown using pulsed laser deposition suggests that the nitrogen species formed in plasma likely correspond to adsorbates on terraces and at extended defects. In the presence of hydrogen, the nitrogen peak reveals significant hydrogenation, and residual gas analysis shows the presence of NH₃ and N₂H_n. In a temperature-dependent study up to 300°C, we detect ammonia in the residual gas at all times, whereas the hydrogenated surface species in XPS spectra decrease with increasing temperature, indicating a shorter residence time or their decomposition.

9:45am **SS+AMS-MoM-7 Velocity Map Imaging of Desorbing Oxygen from sub-Surface States of Single Crystals**, A. Dorst, R. Dissanayake, Georg-August Universität, Göttingen, Germany; D. Killelea, Loyola University Chicago; Tim Schäfer, Georg-August Universität, Göttingen, Germany

We combine velocity map imaging (VMI) with temperature-programmed desorption (TPD) and molecular beam surface scattering experiments to record the angular-resolved velocity distributions of recombinatively-desorbing oxygen from single crystal surfaces. We assign the velocity distributions to desorption from specific surface and sub-surface states by matching the recorded distributions to the desorption temperature. These results provide insight into the recombinative desorption mechanisms and the availability of oxygen for surface-catalyzed reactions. We use concepts of detailed balance to analyze translational energy distributions of O₂ when shifted towards hyperthermal energies. These distribution indicate desorption from intermediate activated molecular chemisorption states.

10:30am **SS+AMS-MoM-10 Designing the Local Environment of Single Atom Catalysts for Product Selectivity: Theory Meets Experiment**, Talat Shahnaz Rahman, University of Central Florida

INVITED

Singly dispersed transition metal atoms on oxide surfaces, the so-called single atom catalyst (SAC) have recently been shown to attain chemical activity and selectivity for several technologically important reactions that surpass those of Pt single crystal surfaces, the prototype exemplary catalyst but with a large price tag. Apart from being cost-effective, single atom catalyst offer excellent opportunities for tuning their local environment and thereby their oxidation state, local coordination, and electronic structure. In this talk, I will present results of collaborative work with several experimental groups on singly-dispersed transition metal atoms anchored on metal oxide surfaces, with and without ligands, that have the potential to be cost-effective catalysts with high activity and product selectivity. Examples will include Pd and Pt atoms anchored on ZnO that form a bimetallic local environment consisting of one Pd and three Zn atoms with high catalytic activity for generation of H₂ through methanol partial oxidation (MPO) [1] and Pt atoms stabilized in specific fine-tuned local coordination environments that exhibit strikingly distinct catalytic behaviors in reactions as varied as CO oxidation and NH₃ oxidation [2]. I will also pay attention to the special role played by ligands (1,10-phenanthroline-5,6-dione (PDO)) in emergent catalytic properties of Pd single atoms stabilized on ceria surfaces [3]. I will also draw attention to some factors that control the emerging functionalities of the above systems in controlled confinement.

[1] Y. Tang, et al., Nano Lett. 20, 6255 (2020); T.B. Rawal, et al., ACS Catalysis 8, 5553-5569 (2018).

[2] W. Tan, et al., Nat Commun. 13, 7070 (2022)

[3] E. Wasim, N. Ud Din, D. Le, et al., J. Catalysis 413, 81 (2022)

* The work is supported by NSF grant CHE-1955343 and performed in collaboration with D. Le, N. U. Din, D. Austin, T. Rawal, T. Jiang, and the research groups of F. Tao (U of Kansas), F. Liu (UCF), S. Tait (Indiana U).

11:00am **SS+AMS-MoM-12 Stabilizing and Characterizing Single-Atom Catalysts: Rhodium on Titania**, Faith J Lewis, M. Eder, J. Hütner, D. Rath, J. Balajka, J. Pavelec, G. Parkinson, TU Wien, Austria

Single-atom catalysis (SAC) aims to minimize the amount of precious metals in catalysts while maintaining catalytic activity. SAC often uses oxide supports to stabilize individual transition metals as isolated active sites. A multi-technique surface science approach allows characterization of these sites to determine their coordination structure. In this work, rhodium adatoms, stabilized by carbon monoxide, were studied on a rutile titania (r-TiO₂(110)) surface.

In idealized SAC systems, metal atoms are assumed to stay isolated on oxide surfaces. In reality, this is not always the case. On titania, rhodium adatoms readily sinter into larger clusters above cryogenic temperatures. It has been suggested that adding ligands stabilizes single rhodium atoms on the surface; carbon monoxide has been proposed to form a geminal dicarbonyl (Rh(CO)₂) structure to stabilize the individual rhodium atoms on r-TiO₂(110).¹

The rhodium gem-dicarbonyl infrared (IR) stretch has been used to signify single rhodium atoms on titania surfaces since the turn of the century, but no scanning probe images have been published of this Rh(CO)₂/r-TiO₂(110) system. Using a newly integrated infrared reflection absorption spectroscopy (IRAS) system, a protocol for forming the Rh(CO)₂ species on r-TiO₂(110) in UHV was established. In this talk, I will present scanning tunneling microscopy (STM) and non-contact atomic force microscopy (nc-AFM) images of the rhodium gem-dicarbonyl system after annealing to various temperatures with complementary IRAS and X-ray photoelectron spectroscopy (XPS) data. The images show two distinct double-lobed species, one parallel to the [001] direction and one perpendicular, at a low coverage (0.005 ML). Contradictory to theoretical predictions,² the images show an asymmetry of the two lobes in both confirmations. Our results illustrate that the surface science approach provides unique information about single atom catalysts and is a prerequisite for their accurate theoretical description.

1. Frank, M.; Bäumer, M.; Kühnemuth, R.; Freund, H.-J., Metal Atoms and Particles on Oxide Supports: Probing Structure and Charge by Infrared Spectroscopy. *The Journal of Physical Chemistry B*, 8569-8576 (2001).

2. Tang, Y., Asokan, C., Xu, M. et al., Rh single atoms on TiO₂ dynamically respond to reaction conditions by adapting their site. *Nature Communications*, 4488 (2019).

11:15am **SS+AMS-MoM-13 In-Situ Observation of the Effects of Oxygen-Containing Compounds on MoS₂-Based Catalysts Using Near-Ambient Pressure Scanning Tunneling Microscopy**, Kerry Hazeldine, M. Hedevar, Aarhus University, Denmark; L. Mohrhusen, Carl von Ossietzky University of Oldenburg, Germany; J. Vang Lauritsen, Aarhus University, Denmark

More than 20% of greenhouse gas emissions in the European Union are produced by the heavy transport and aviation sector. Pyrolysis oil derived from biomass is a promising replacement for fossil fuels for aviation and heavy transport applications and is one of the technologies being researched for the generation of green aviation fuel. Fast pyrolysis is a process of decomposing biomass into pyrolysis oil by rapidly heating it in an oxygen-free atmosphere. An advantage of pyrolysis oil derived from biomass is that it is compatible with the existing infrastructure that is used in the catalysis and distillation of jet fuels and diesel. However, the oxygen content in pyrolysis oil derived from biomass is unacceptably high (up to 50%) and can lead to corrosion and instability [1].

To reduce the oxygen content and produce useful and efficient hydrocarbons from the pyrolysis oil, a pre-treatment and hydrodeoxygenation (HDO) step is required to be added to the refining process. Molybdenum disulphide (MoS₂) has previously demonstrated its effectiveness as a catalyst in hydrodesulphurisation (HDS) and has further shown to be a promising candidate as a catalyst in HDO and is therefore the primary material of interest in this study [2].

To develop atomistic structure determination of the catalyst and elucidate to the reaction pathways for oxygen-containing molecules during HDO, model studies are required. In this study, the model system based on MoS₂ growth on Au(111), has been exposed to oxygen-containing molecules and characterised in-situ using the surface-sensitive techniques, near-ambient pressure scanning tunnelling microscopy (NAP-STM), and near-ambient pressure X-ray photoelectron spectroscopy (NAP-XPS). By using a gold substrate, the oxygen uptake can be evaluated without background from the oxide support. NAP-XPS shows evidence of O exchange on the sulphide phase, consistent with current theoretical models, whilst the corresponding NAP-STM shows structural changes to the particle shape and size of the sulphide phase. For example, preliminary work shows restructuring in the MoS₂ clusters when exposed to elevated pressures of methanol vapour. By using these complementary techniques, we can gain insight into both the chemical and physical changes of MoS₂ upon exposure to oxygen-containing compounds.

late transition metal nanoparticles across oxides streamlines development of optimal catalysts.

[1] Cao J, Zhang Y, Wang L, Zhang C, Zhou C. Unsupported MoS₂-Based Catalysts for Bio-Oil Hydrodeoxygenation: Recent Advances and Future Perspectives. *Front Chem.* 10, 928806 (2022).

[2] Salazar, N., Rangarajan, S., Rodríguez-Fernández, J. *et al.* Site-dependent reactivity of MoS₂ nanoparticles in hydrodesulfurization of thiophene. *Nat Commun.* 11, 4369 (2020).

11:30am **SS+AMS-MoM-14 Revealing Local Coordination of Ag Single Atom Catalyst Supported on CeO₂(110) and ZrO₂(-111), Syeda Sherazi, D. Le, K. Ye, S. Xie, F. Liu, T. Rahman, University of Central Florida**

Single atom catalyst (SAC) supported on metal oxide surfaces is a promising candidate for various reactions as it possesses high temperature stability and potentially high selectivity. Determining the local atomic coordination and geometric structure of the SAC is important for the understanding of its catalytic performance. In this work, we apply the ab initio thermodynamics approach to investigate the coordination environment of Ag SAC supported on CeO₂(110) and ZrO₂(-111), so chosen as accompanying experimental observations find the former to be a more viable support than the latter. We find that the Ag SAC structure in which Ag is embedded in the CeO₂ lattice with one surface oxygen vacancy nearby is the most favorable on the CeO₂(110) surface while the structure in which Ag embeds in the ZrO₂(-111) lattice without any oxygen vacancy nearby is the most favorable on the ZrO₂(-111) surface. Our results also show that it is easier to create oxygen vacancy near the Ag atom when the support is CeO₂(110) than ZrO₂(-111). We compare the trends in the energetics of NH₃ adsorption and dissociation on Ag SAC supported on CeO₂(110) with those on ZrO₂(-111) to compare with accompanying experimental observations that find the ceria-supported Ag SAC to exhibit a pronounced selectivity in ammonia oxidation. We will report experimental data to compare with our finding and comment on their implications for the catalytic performance of the Ag SAC.

Work is supported by National Science Foundation grant CHE-1955343.

11:45am **SS+AMS-MoM-15 Trends for Predicting Adhesion Energies of Catalytic Late Transition Metal Nanoparticles on Oxide Supports, Nida Janulaitis, The University of Washington; K. Zhao, C. Campbell, University of Washington**

Understanding the energetics of late transition metal nanoparticles dispersed on oxide-based catalyst support materials is important for the development of high-performance catalysts. Metal/support adhesion energies, which are used to estimate the metal chemical potential as a function of metal nanoparticle size, which in turn correlates with the surface reactivity and sintering kinetics of the metal nanoparticles. Single crystal adsorption calorimetry (SCAC) was used to directly measure Cu vapor adsorption energies and Cu chemical potential as a function of Cu coverage on the clean rutile-TiO₂(100) surface, while He⁺ low-energy ion scattering (LEIS) was used to measure the average size of the Cu nanoparticles. By fitting these data to a theoretical model, we extracted the adhesion energy of Cu nanoparticles on rutile-TiO₂(100). By comparing to earlier results for Ag, we find that the adhesion energies of metals on the rutile-TiO₂(100) surface correlate proportionally to the oxophilicity of the metal element. Similar proportional correlations for the adhesion energy of metals to MgO(100) and CeO₂(111) surfaces as a function metal oxophilicity have been previously published. Expanding upon these existing oxide adhesion energy trends with the new rutile-TiO₂(100) data clarifies the structure-function relationship between the physical properties of the oxide supports and their metal adhesion energetics. The ability to predict the adhesion energy, and thus the metal chemical potential versus size, of

Surface Science

Room 120 - Session SS+AMS-MoA

Surface Chemistry and Reactivity on Oxide Surfaces

Moderators: Ashleigh Baber, James Madison University, J. Anibal Boscoboinik, Center for Functional Nanomaterials, BNL

1:30pm SS+AMS-MoA-1 Dynamic Formation of Gem-Dicarbonyl on Rh Decorated Fe₃O₄(001), Jiří Pavelec, C. Wang, P. Sombut, L. Puntischer, M. Eder, Vienna University of Technology, Austria; Z. Jakub, CEITEC, Czechia; R. Bliem, Advanced Research Center for Nanolithography, Netherlands; M. Schmid, U. Diebold, Vienna University of Technology, Austria; C. Franchini, University of Vienna, Austria; M. Meier, G. Parkinson, Vienna University of Technology, Austria

Single atom catalysts (SACs) have the potential to reduce the amount of precious materials needed in catalytic reactions. Understanding and utilizing SACs requires studying the coordination of adatoms to their supports, as well as their coordination to reactants. This coordination can change during reactions, and intermediate dynamic steps may be invisible to conventional spectroscopy.

In this study [1], we employ scanning tunneling microscopy (STM) in combination with theory to investigate a model SAC: Rhodium decorated Fe₃O₄(001). Our results demonstrate that the formation of dicarbonyl on Rh₁ requires the initial presence of Rh₂ on the surface, a finding corroborated by detailed density functional theory (DFT) studies.

CO adsorption at Rh₁ sites at room temperature results exclusively in stable Rh₁CO monocarbonyls, as the Rh atom adapts its coordination to form a stable pseudo-square planar environment. Rh₁(CO)₂ gem-dicarbonyl species are also observed, but they form exclusively through the break up of Rh₂ dimers via an unstable Rh₂(CO)₃ intermediate. Identification of this intermediate step would be challenging without a multi-technique approach.

These results are compared to the Rh decorated TiO₂ model SAC using temperature-programmed desorption (TPD), infrared reflection absorption spectroscopy (IRAS) [2], nc-AFM, and X-ray photoelectron spectroscopy (XPS).

[1] Wang, C.; Sombut, P.; Puntischer, L.; Jakub, Z.; Meier, M.; Pavelec, J.; Bliem, R.; Schmid, M.; Diebold, U.; Franchini, C.; Parkinson, G. S., *Angewandte Chemie* **2024**, 63 (16).

[2] Rath D.; Mikerásek V., Wang C.; Eder M.; Schmid M.; Diebold U.; Parkinson G.S., Pavelec J. **2024**, *submitted*

1:45pm SS+AMS-MoA-2 Water-Gas Shift Reaction Mechanisms on Ligand Coordinated Pt Single Atom Catalyst: Insights from DFT & Microkinetics, Dave Austin, D. Le, T. Rahman, University of Central Florida

Hydrogen is a promising renewable and environmentally friendly fuel to meet future global energy needs. An important reaction to produce hydrogen is the water-gas shift (WGS) reaction, (CO+H₂O→CO₂+H₂; ΔH=-41.1 KJ/mol). Interest in the use of single-atom catalysts (SACs) for facilitating these reactions has grown. This project explores a new strategy that can create a metal-ligand coordinated SAC on metal oxide (Titanium oxide) support. 1,10-phenanthroline-5,6-dione (PDO), was chosen as the ligand for its oxidative potential for stabilizing metal cations in two bidentate sites. Our experimental collaborators Fereshteh Rezvani and Steve Tait from Indiana University were able to characterize the single-atom nature of the Pt with EXAFS, XPS, XRD, DRIFTS, and TEM. They evaluated for the WGS reaction, and it was discovered that Pt-ligand SAC supported on defective TiO₂ shows higher inherent catalytic activity than Pt NPs with significantly lower activation energy which is generally desirable for the redox mechanism.

First, the structure of the Pt-PDO molecule had to be determined, this is because the ligand has two bidentate sites. Experimental results that this complex has a ratio of 2:1 for the ligand to Pt, giving three different potential structures. After the molecule was determined, we had to understand the role of vacancies on the TiO₂ surface. The Pt-PDO complexes (all three configurations) were adsorbed onto to TiO₂ surface that was either clean, or had an oxygen, titanium, or oxygen and a titanium vacancy. We showed that the vacancies were important to activate the Pt-PDO complex, on the clean surface there is only van der Waals interaction between the surface and the complex. The electronic structure of these systems also shows the activation of the Pt atom from vacancies, as the Pt becomes more reactive and has its frontier orbitals pushed closer to the

Fermi level. The WGS reaction has two different proposed mechanisms. They are the Redox and the associative mechanisms. They differ by which point the reactants are adsorbed. These two mechanisms' pathways were simulated on the Pt-PDO complex and to understand the role of ligands the Redox mechanism was also studied on a single Pt atom. The DFT calculations confirmed that the redox mechanism has a lower energy barrier than the associative mechanism for Pt-ligand SAC. A microkinetic study was also performed to obtain the theoretical turnover frequency for all three reactions. The microkinetic study shows that the Redox mechanism has a higher turnover frequency than that of the associative and single Pt atom reactions.

2:00pm SS+AMS-MoA-3 Surface Chemistry and Catalysis of IrO₂(110), Jason Weaver, University of Florida; A. Asthagiri, Ohio State University; M. Kim, Yeungnam University, Republic of Korea; J. Jamir, C. Pope, University of Florida; J. Yun, Ohio State University; S. Ramasubramanian, University of Florida

INVITED

Developing more efficient catalytic processes to oxidize light-alkanes partially or completely is important for various applications, including power generation, exhaust gas remediation and chemical synthesis. In this talk, I will discuss investigations of alkane oxidation on the IrO₂(110) surface, and emphasize how mechanistic insights obtained from UHV surface science experiments and DFT calculations have been used to inform our understanding of rates and species coverages measured during alkane oxidation under catalytic conditions. I will discuss the development of a first-principles microkinetic model that accurately reproduces key aspects of the kinetics of methane oxidation on IrO₂(110) and identifies how different surface species, observed using operando spectroscopy, affect the catalytic kinetics. I will also discuss recent results which clarify how gaseous H₂O influences the catalytic oxidation of ethane on IrO₂(110) and the surface species that develop under reaction conditions. Our studies demonstrate how fundamental knowledge gained from surface science and DFT calculations can play a critical role in interpreting operando measurements and identifying the mechanisms of complex, catalytic reactions.

2:30pm SS+AMS-MoA-5 Room Temperature Activation of Methane and Its Dry Reforming by MgO Nanostructures Embedded in CuO_x on Cu(111), Areebin Islam, K. Reddy, Brookhaven National Laboratory; Y. Tian, Stony Brook University/Brookhaven National Laboratory; J. Rodriguez, Brookhaven National Laboratory

Natural gas, primarily methane, is valued for its versatility and potential in sustainable energy production through reforming or partial oxidation reactions. The investigation stems from the need for efficient technologies to utilize natural gas for sustainable syn gas or hydrogen production while simultaneously addressing carbon dioxide (CO₂) utilization and conversion challenges. MgO nanostructures show promise for methane activation due to their unique surface properties, while Cu-based catalysts are explored for selective methane oxidation at lower temperatures. This study investigates the growth and reactivity of MgO nanostructures on a Cu₂O/Cu(111) substrate, employing scanning tunneling microscopy (STM) and synchrotron-based ambient-pressure X-ray photoelectron spectroscopy (AP-XPS). Deposition of Mg atoms on the "29" structured copper oxide film induces oxygen transfer from the Cu₂O/Cu(111) substrate to the deposited Mg, forming MgO and CuO_x. Diverse morphologies are observed, including structured copper oxide films with embedded MgO clusters (1-3 Mg atoms) and randomly dispersed MgO nanoparticles. Reactivity studies reveal that MgO nanostructures smaller than 1 nm in width activate methane at room temperature, dissociating it into CH_x species. CO₂ dissociates into CO and C species instead of forming plain carbonates. The size and morphology of MgO nanostructures significantly influence their reactivity, enabling dry reforming of methane (MDR) by CO₂ into syn gas. Specifically, MgO nanostructures with a coverage of 0.04-0.11 ML activate methane at room temperature, leading to its dissociation into CH_x species. Additionally, smaller MgO clusters (0.2-0.5 nm in width, 0.4-0.6 Å in height) at lower coverages exhibit distinct reactivity towards CO₂, dissociating it into CO and C species. This investigation underscores the size- and morphology-dependent reactivity of MgO nanostructures, showcasing a behavior distinct from bulk MgO. The catalytic performance observed is attributed to the unique magnesium-copper interface, featuring multifunctional sites comprising magnesium cations, oxygen, and copper cations, which facilitate methane activation and drive the MDR processes forward at around 500K.

Monday Afternoon, November 4, 2024

2:45pm **SS+AMS-MoA-6 Mixed IrO₂/RuO₂(110) Thin Films: Distinct Surface Chemical Properties of the Single-Layer Oxides**, *Suriya Narayanan Ramasubramanian, C. Sudarshan, J. Shin, C. Lee*, University of Florida, Gainesville; *C. Plaisance*, Louisiana State University; *D. Hibbitts, J. Weaver*, University of Florida, Gainesville

Mixed metal-oxides of IrO₂ and RuO₂ have potential to serve as efficient catalysts for promoting the partial or complete oxidation of alkanes, due to the unusual ability of IrO₂ to activate light alkanes at low temperature as well as the possibility that the mixed oxides exhibit distinct surface chemical properties compared with the pure oxides. In this talk, I will discuss our recent studies of the growth and surface chemical properties of layered structures of IrO₂(110) and RuO₂(110) thin films as well as mixed IrO₂-RuO₂(110) films prepared in UHV. We find that single-layers (SL) of IrO₂(110) on RuO₂(110) and vice versa exhibit distinct binding properties toward adsorbed molecules compared with the corresponding multilayer (ML), bulk-like oxides. TPD shows that the binding of N₂ and O is stronger on SL-RuO₂(110) on ML-IrO₂(110) relative to ML-RuO₂(110), whereas these species bind more weakly on SL-IrO₂(110) on ML-RuO₂(110) relative to ML-IrO₂(110). These differences are especially pronounced for oxygen in that the binding energy of an adsorbed O-atom on top of a surface metal site increases in the order, SL-IrO₂ < ML-RuO₂ < ML-IrO₂ < SL-RuO₂, with the binding energy differing by ~50 kJ/mol between each single vs. multiple layer structure. I will discuss DFT calculations which show that these differences originate from a trans-ligand effect, wherein the bonding properties of surface metal atoms are strongly influenced by the bonding of sub-surface O-atoms to the second layer oxide. Lastly, I will discuss recent results showing that well-mixed Ir_xRu_yO₂(110) thin films can be generated in UHV and will discuss their surface chemical properties. The significant differences between the surface chemical properties of single vs. multiple layer oxide structures may have broad implications for understanding the catalytic behavior of mixed IrO₂/RuO₂ systems.

3:00pm **SS+AMS-MoA-7 Active Sites for Oxidation Reactions on Cu₂O Surfaces**, *Dario Stacchiola*, Brookhaven National Laboratory

Cu-based catalysts are active for partial and full oxidation reactions. Copper can be oxidized under moderate oxidant pressures and temperature to Cu₂O, and further to CuO under typical catalytic reaction conditions. We present here model systems using both copper oxide thin films and single crystals used to interrogate the effect of modifiers on the stability of exposed active Cu sites. *In situ* experiments allow the observation of dynamic processes and phases under reaction conditions.

References

- [1] "Oxidation of CO on a reconstructed Cu₂O surface", (submitted)
- [2] "Stabilization of Cu₂O through site-selective formation of a Co₂Cu hybrid single-atom catalyst", *Chem. Mat.* **34**,2313(2022)
- [3] "Potassium-Promoted Reduction of Cu₂O/Cu(111) by CO", *J. Phys. Chem. C* **123**, 8057–8066 (2019)
- [4] "Redox Properties of Cu₂O(100) and (111) Surfaces", *J. Phys. Chem. C* **122**, 28684–28691 (2018)

3:15pm **SS+AMS-MoA-8 Tracking Elementary Steps in Conversion of Carboxylic Acids on Single Crystalline and Nanofaceted TiO₂(101)**, *Xingyu Wang*, Pacific Northwest National Lab; *W. Debenedetti*, Los alamos National Laboratory; *C. O'Connor*, Harvard University; *Z. Dohnalek, G. Kimmel*, Pacific Northwest National Lab

Ketonization of carboxylic acid used to be a method to produce acetone in industry. Recent interest has focused on this C-C coupling reaction due to its potential for upgrading biomass. The production of acetone from acetic acid was only observed in high pressure reactors on anatase nanoparticles. However, on anatase TiO₂(101) single crystals in ultra-high vacuum (UHV), acetone production from acetic acid has not been observed. This is an example of the material gap in surface science studies. The mechanism of ketonization is also under debate; the two most commonly proposed pathways are β-keto acid pathway and ketene pathway.

In this study, we introduced well-defined nanoparticles (NPs) with mostly (101) surfaces into a UHV chamber to elucidate the ketonization mechanism and bridge the material and pressure gaps in this system. A combined experimental approach of temperature programmed desorption (TPD), scanning tunneling microscopy (STM), X-ray photoelectron spectroscopy (XPS), and reflection absorption infrared spectroscopy (RAIRS) was used, along with theoretical studies. Our finding is that on single crystals, the ketene produced desorbs from the surface without encountering another acetate. In contrast, ketene desorbing from a given NP within a layer of NPs can subsequently react with an acetate on another

NP, leading to acetone production. To demonstrate this, we prepared three samples with varying thickness of anatase NP layers, with mostly (101) facets, in an UHV system. We then compared the reaction of acetic acid on these NP layers with its reaction on an anatase(101) single crystal. We found that the production of acetone starts from 10ML of acetic acid exposure, and the yield correlates with the depth of acetic acid absorption into the nanoparticle beds. Along with theoretical studies, we identified a mechanism through a key intermediate, α-enolate acetic acid, which forms through the reaction of gas phase ketene with surface-bound acetate species. Further studies, which involve dosing ketene through a homemade heated quartz tube ketene source onto an acetic acid pre-dosed single crystal surface, are currently underway to confirm this reaction mechanism.

3:30pm **SS+AMS-MoA-9 Developing First-principles Microkinetic Models for Selective Ethane Oxidation on Cl-substituted IrO₂(110)**, *Jungwon Yun*, The Ohio State University; *D. Bae, N. Park*, Yeungnam University, Republic of Korea; *J. Weaver*, University of Florida; *M. Kim*, Yeungnam University, Republic of Korea; *A. Asthagiri*, The Ohio State University

In this study, we investigated the role of Cl doping on ethylene selectivity for ethane oxidation on IrO₂(110) using a combination of density functional theory (DFT) and microkinetic modeling (MKM). Catalytic oxidative dehydrogenation (ODH) of ethane is an attractive route to produce value-added products such as ethylene. Our previous research demonstrated that stoichiometric IrO₂(110) exhibits significant potential for ethylene production at low temperature (~ 400 K) due to the low activation energy for initial C-H bond cleavage of light alkanes. Temperature programmed reaction spectroscopy (TPRS) experiments showed that surface HO groups promote ethylene selectivity in ethane ODH. Given Cl is isoelectronic to surface HO groups and has been experimentally shown to be able to substitute bridge O atoms on RuO₂(110) surfaces, we explored Cl substitution effects on ethylene selectivity on IrO₂(110). DFT calculations indicated that the presence of bridge Cl on the IrO₂(110) surface destabilizes adjacent adsorbed ethane and ethylene but has minimal impact on the reaction barriers of C₂H_x species with adjacent oxygen. This suggests that limited Cl substitution would still allow the IrO₂(110) surface to convert C₂H₆ to C₂H₄, but subsequently start to constrain further dehydrogenation and oxidation steps due to the lack of bridge O atoms. A DFT-based MKM was developed to understand the relationship between product yields (C₂H₆, C₂H₄, CO/CO_x) on degree of Cl substitution. The MKM modeled TPRS confirms that ethylene yield is increased by Cl substitution but eventually reaches a maximum where there is a drop due to the deactivation of the surface. This maximum in ethylene yield is dependent on initial C₂H₆ coverage since dehydrogenative oxidation steps produce surface HO groups that, when combined with bridge Cl, deactivate the surface. We will discuss ongoing work to extend the MKM simulations to reaction conditions where activity and selectivity are examined as a function of partial pressures of C₂H₆ and O₂ along with percent Cl substitution.

4:00pm **SS+AMS-MoA-11 Small Alcohol Reactivity Over TiO₂/Au(111) Inverse Model Catalysts**, *Ashleigh Baber*, James Madison University

Gold-based catalysts have received tremendous attention as supports and nanoparticles for heterogeneous catalysis, in part due to the ability of nanoscale Au to catalyze reactions at low temperatures in oxidative environments. Surface defects are known active sites for low temperature Au chemistry, so a full understanding of the interplay between intermolecular interactions and surface morphology is essential to an advanced understanding of catalytic behavior and efficiency. Our undergraduate research lab uses ultrahigh vacuum temperature programmed desorption (UHV-TPD) to investigate the fundamental interactions between small alcohols on Au(111) and the reactivity of TiO₂/Au(111) inverse model catalysts on small alcohol redox behavior. In a systematic study to better understand the adsorption and intermolecular behavior of small alcohols (C₁-C₄) on Au(111) defect sites, coverage studies of methanol, ethanol, 1-propanol, 1-butanol, 2-butanol, and isobutanol have been conducted on Au(111). These small alcohols molecularly adsorb on the Au(111) surface and high resolution experiments reveal distinct terrace, step edge, and kink adsorption features for each molecule. The desorption energy of small primary alcohols was shown to trend linearly with increasing C₁-C₄ carbon chain length, indicating that the H-bonded molecular packing of 1-butanol resembles that of methanol, ethanol, and 1-propanol, while isobutanol and 2-butanol deviate from the trend. These energy insights are particularly interesting when studying the redox behavior of small alcohols over TiO₂/Au(111). Depending on the surface preparation conditions, Au(111) supported TiO₂ nanoparticles react with

Monday Afternoon, November 4, 2024

small alcohols to form either reduced and oxidized products. The reactivity of the surface for ethanol oxidation was altered by controlling the oxidation state of TiO_x ($x < 2$) and coverage of TiO_2 . Low coverages of fully oxidized TiO_2 nanoparticles on Au(111) are active for the selective oxidation of ethanol to form acetaldehyde, but not all small alcohols behave similarly.

4:15pm **SS+AMS-MoA-12 Partial Chlorination of IrO_2 (110) for Selective Ethane Chemistry**, Connor Pope, University of Florida, Gainesville; J. Yun, Ohio State University; R. Reddy, J. Jamir, University of Florida, Gainesville; M. Kim, Yeungnam University, Republic of Korea; A. Asthagiri, Ohio State University; J. Weaver, University of Florida, Gainesville

Developing more efficient catalytic processes to convert ethane to ethylene is important for improving hydrocarbon-to-chemicals processing and transitioning to carbon-neutral technologies. Our prior work demonstrates that C_2H_6 dehydrogenation on the IrO_2 (110) surface produces C_2H_4 between ~350 and 450 K during temperature programmed reaction spectroscopy (TPRS), and that the C_2H_4 selectivity can be increased by pre-hydrogenating the oxide surface to deactivate a fraction of the surface oxygen sites. In this talk, I will discuss recent work in which we controllably replaced surface O-atoms of IrO_2 (110) with Cl-atoms through the oxidation of gaseous HCl in ultrahigh vacuum. We find that the stepwise adsorption of HCl on IrO_2 (110) with heating to 650 K causes H_2O desorption, and generates Cl atoms on bridging and on-top sites in about a 1:1 ratio, with the total Cl coverage saturating near 0.7 ML. Measurements using TPRS and XPS further demonstrate that the partitioning of Cl-atoms between bridging and on-top sites can be altered by exposing the surfaces to reducing vs. oxidizing conditions. Lastly, I will discuss how partial chlorination affects the surface reactivity toward CO and C_2H_6 , and produces a nearly two-fold increase in the selectivity of C_2H_6 dehydrogenation to C_2H_4 during TPRS. Our findings demonstrate the potential of controlled surface deactivation for improving the selectivity of IrO_2 (110) for partial alkane oxidation.

4:30pm **SS+AMS-MoA-13 Insights into CO_2 Hydrogenation on the InO_x/Cu (111) and InO_x/Au (111) Surfaces: Surface Electronic Structure and Reaction Mechanistic Studies**, Prabhakar Reddy Kasala, J. Rodriguez, Brookhaven National Laboratory

In CO_2 hydrogenation, In_2O_3 catalysts are known for their higher CH_3OH selectivity, primarily attributed to their oxygen vacancies. Subsequent studies explored depositing metals on In_2O_3 to enhance CO_2 conversion and oxygen vacancy formation.^{1,2} Besides metal supported on In_2O_3 -based catalysts, intermetallic In-M (M= Pd, Cu) compounds have also shown good performance for CO_2 hydrogenation to methanol synthesis.^{3,4} Despite extensive research on metal (M) supported In_2O_3 catalysts, the role of In-M alloy and M/ In_2O_3 interfaces in CO_2 activation and methanol selectivity remains unclear. Our surface electronic structural studies using APXPS reveal that during CO_2 hydrogenation, very low coverage (~0.035 ML) InO_x/Cu (111) undergoes structural changes at/above 500 K, forming a Cu-In intermetallic alloy at the surface. Further increase in Indium coverage (0.325 ML) results in InO_x/Cu (111) at the surface, while the interface remains an In-Cu alloy. Carbon 1s core level spectra of the InO_x/Cu (111) regions of the surface under 1 Torr of $\text{CO}_2 + \text{H}_2$ (1:3 ratio) show the formate (HCOO^*) and H_xCO^* species, with H_xCO having the higher concentration at 500 K in 0.035 ML, while the 0.325 ML Indium oxide has shown the carbonate (CO_3^*) at 300 K and decreased with an increase in temperature to 500 K. Our results clearly demonstrate the promotional effects of In_2O_3 for CO_2 hydrogenation. Furthermore, we extended our studies on InO_x/Au (111) and $\text{InO}_x/\text{TiO}_2$ (001) surfaces to understand the role of Oxide/Metal, Alloy, Oxide/Oxide roles in methanol selectivity. Our preliminary STM and XPS results on InO_x/Au (111) established the preparation of In/Au (111) and InO_x/Au (111) surfaces. We are making progress on indium-based catalysts for CO_2 hydrogenation to establish the role of possible alloys/intermetallic and metal-support interfaces in CO_2 activation and CO_2 hydrogenation to methanol under reaction conditions.

References:

1. Cao et. al., *ACS Catal.* 2021, 11, 1780-1786
2. Rui et. al., *ACS Catal.* 2020, 10, 11307-11317
3. Shi et. al., *J. Catal.* 2019, 379, 78-89
4. Chen et. al., *ACS Catal.* 2019, 9, 8785-8797

4:45pm **SS+AMS-MoA-14 Structural-Electronic Property Evolution of LiCoO_2 (001) Under Varied Oxygen Chemical Potentials**, Yuchen Niu, J. Reutt-Robey, University of Maryland College Park

Since its discovery as an intercalation Li-ion battery electrode in 1980, LiCoO_2 remains a popular cathode material for portable devices. Its surfaces also provide an unexplored opportunity to tune the structure and charge-

Monday Afternoon, November 4, 2024

transport properties for emergent electronic applications. In this study, we report on the evolution of LiCoO_2 (001) surfaces, specifically their structural and electronic property response to processing under low/high O_2 chemical potential extremes via scanning probe microscopy (SPM), low energy electron diffraction (LEED), X-ray photoelectron spectroscopy (XPS) and Raman spectroscopy.

Under a traditional UHV regimen at low O_2 chemical potentials, LiCoO_2 (100) persistently displays a diffused (1x1) LEED pattern after many cycles of Ar^+ sputtering- thermal annealing, suggestive of nanoscale disorder without major atomic surface reconstruction. UHV-STM imaging reveals the singular surface terminated by shallow grains of ~2 nm width, which coarsen to ~30 nm grains under prolonged processing. Atomically resolved images of local regions show ($\sqrt{7} \times \sqrt{7}$) R 19.1° ordering, which could be attributed to local Li ordering on Li-terminated layers. The electronic properties of this surface are further mapped with UHV scanning tunneling spectroscopy. Electronic band gaps derived from I-V spectroscopy are reported. This is corroborated by in situ XPS measurements of the surface chemical composition and valence band structures during the Ar^+ sputtering- thermal annealing cycles.

Under high O_2 chemical potentials (160~ 760 torr O_2), dramatic changes in surface structures are observed, indicating more efficient surface mass transport. In contrast to the nanograin features observed at low O_2 chemical potentials, high O_2 chemical potential treatments generate expansive atomically flat (100) terraces of ~ 1 μm width, step edges and quasi-hexagonal islands. Partial surface decomposition to Co_3O_4 due to Li loss is also observed.

Surface Science

Room 120 - Session SS+2D+AMS-WeM

On-Surface Synthesis: Atomic and Molecular Ensambling on Surfaces

Moderators: Irene Groot, Leiden University, The Netherlands, Nan Jiang, University of Illinois - Chicago

8:00am **SS+2D+AMS-WeM-1 On-surface Synthesis of Porous Graphene Nanoribbons**, T. Qin, Junfa Zhu, University of Science and Technology of China **INVITED**

The low-dimensional porous graphene nanomaterials might have intriguing electronic properties and open exciting possibilities in the field of functional materials. By using rationally designed precursor molecules, on-surface synthesis approach has emerged as a powerful platform for the synthesis of porous low-dimensional graphene-based nanostructures with atomic precision. In this presentation, we report our recent work on the synthesis of porous graphene nanoribbon and nanosheet on different metal surfaces. We have successfully synthesized the one-dimensional graphene nanoribbons (GNRs) containing periodic [14]annulene pores on Ag(111) and the two-dimensional graphene nanosheets containing periodic [30]annulene pores on Au(111), originating from a same precursor. Two distinct reaction pathways on the two surfaces were regulated by different thermodynamic and kinetic mechanisms. With the combination of the scanning tunneling microscopy, synchrotron radiation photoemission spectroscopy and density functional theory (DFT) calculations, we identified the reaction products, intermediates precisely, and obtained insights into the reaction mechanism. On Ag(111), the formation of porous GNR is a thermodynamically favored pathway, by going through a flexible and reversible organometallic intermediate state. In contrast, on Au(111), because the debromination process is the rate-limiting step for the covalent coupling reaction and the generated covalent structures are irreversible, giving rise to the hierarchical formation of covalent chains and 2D porous nanosheet. The reaction mechanisms were confirmed by a series of control experiments, and the appropriate thermodynamic and kinetic parameters for optimizing the reaction pathways were proposed. Furthermore, DFT calculations revealed the influence of surface confinement on the band structures of these two nonplanar pores embed carbon materials, which enhances the conjugation of π -electrons thus shrinking the band gap.

8:30am **SS+2D+AMS-WeM-3 Tailoring Pt-Based Organometallic Nanomesh on Ag(111): A Model System for “Host-Guest” Chemistry**, V. Carreño-Díaz, A. Ceccatto, E. Ferreira, Abner de Siervo, University of Campinas (UNICAMP), Brazil

On-surface synthesis has been extensively used to produce complex functional nanostructures, such as Metal-Organic Frameworks (MOFs). MOFs are composed of highly ordered molecular structures, where metal adatoms act as connecting nodes, generating porous structures that exhibit a long-range order, offering a favorable environment for the adsorption and reaction of molecules in confined spaces, the so-called “host-guest” chemistry [2]. In the present work, we have studied the formation of bidimensional porous networks with hexagonal geometry (nanomesh) resulting from the combination of two molecular precursors: 1,3,5-tris[4-(pyridin-4-yl)-[1,1'-biphenyl]]benzene (TPyPPB) and dichloro-(1,10-phenanthroline)-platinum(II) (Cl_2PhPt), deposited on the surface of Ag(111). Our results reveal that when the TPyPPB molecules are deposited on the Ag(111) surface, they adopt a porous arrangement with triangular packing mediated by hydrogen bonds [3]. On the other hand, in the presence of the Cl_2PhPt molecule, the chemical interactions between both molecules change upon annealing at 400K, which leads to various ordering patterns before stabilizing in a network with hexagonal geometry. After dehalogenation, the Cl_2PhPt molecule is transformed into a new complex, PhPt, maintaining the Pt atom in its structure. The Cl atoms dissociated from the Cl_2PhPt precursor decorate the periphery of TPyPPB molecules. PhPt molecules can interconnect TPyPPB molecules through metallic coordination between the Pt atom and the N from the pyridyl group (N–Pt–N). The present investigation is based on room temperature scanning-tunneling microscopy (STM) measurements. This experimental approach allows us to explore the properties and structure of these materials at the atomic and molecular levels, opening new perspectives on the design and properties of MOFs.

Acknowledgments:

This work was financially supported by FAPESP (2022/12929-3), CNPq, and CAPES from Brazil.

1. Barth, J., Costantini, G. & Kern, K. Engineering atomic and molecular nanostructures at surfaces. *Nature* 437, 671–679 (2005).

2. Marta Viciano-Chumillas, et al. “Metal-Organic Frameworks as Chemical Nanoreactors: Synthesis and Stabilization of Catalytically Active Metal Species in Confined Spaces”. *Accounts of Chemical Research* 53 (2020) 520–531.

3. Alisson C. dos Santos, Vanessa Carreño-Díaz, et al. “On-Surface Design of Two-Dimensional Networks through Nonmetal Atoms” (under preparation).

8:45am **SS+2D+AMS-WeM-4 Modulating the Reactivity of “Single-Atom Catalyst” Sites Within 2D Metal-Organic Frameworks by Small Structural Distortions**, Zdenek Jakub, CEITEC - Central European Institute of Technology, Czechia; J. Planer, D. Hruza, A. Shahsavar, P. Prochazka, J. Cechal, CEITEC, Czechia

Detailed atomic-scale understanding is a crucial prerequisite for rational design of next-generation single-atom catalysts (SACs). However, the sub-ångström precision needed for systematic studies is difficult to achieve on working SACs. We present a 2D metal-organic system featuring Fe-N_4 single-atom sites,^{1,2} in which the height of the atomically-defined structure is modulated by the 0.4 Å corrugation of the inert graphene/Ir(111) support. We show that the support corrugation significantly affects the system reactivity, as the sites above the support “valleys” bind TCNQ (tetracyanoquinodimethane) much stronger than the sites above the “hills”.³ The experimental temperature stability of TCNQ varies by more than 60 °C on these seemingly identical sites. We expect that similarly strong effects of sub-ångström structural distortions will likely take place whenever large molecules interact with neighboring “single-atom catalyst” sites or when multiple reactants co-adsorb on such sites.

References

[1] Z. Jakub, A. Shahsavar, et al., *JACS*, **146**, 3471–3482 (2024)

[2] Z. Jakub, A. Kurowská, et al., *Nanoscale*, **14**, 9507-9515 (2022)

[3] Z. Jakub, J. Planer, et al., in preparation

9:00am **SS+2D+AMS-WeM-5 On-Surface Synthesis of Polycyclic Heteroatom-Substituted Nanocarbon Materials**, Willi Auwärter, Technical University of Munich, Germany **INVITED**

On-surface synthesis protocols provide elegant routes to individual molecular complexes, oligomers, and other nanocarbon materials on metal supports [1]. The resulting structural, physical, and chemical properties can be controlled by heteroatom-substitution.

In this talk, I will present an overview of our activities employing temperature-induced reactions on coinage metal supports in an ultrahigh vacuum environment, affording specific porphyrinoids and BN-substituted nanocarbon materials. On the one hand, routes to unsubstituted, square-type porphyrin tetramers [2] and peripherally O-doped porphyrins are addressed. On the other hand, dehydrogenation processes of borazine [3] and BN-functionalized carbon scaffolds will be discussed, in view of the synthesis and potential transfer of two-dimensional BNC materials.

[1] Grill, L.; Hecht S. *Nat. Chem.* **2020**, *12*, 115.

[2] Corral Rascon, E. *et al.* *J. Am. Chem. Soc.* **2023**, *145*, 967.

[3] Weiss, T. *et al.*, *Adv. Mat. Interfaces* **2024**, *11*, 2300774

9:30am **SS+2D+AMS-WeM-7 Atomic-Scale Investigation of the Highly Enantiospecific Decomposition of Tartaric Acid on Chiral Cu Surfaces**, Avery Daniels, C. Sykes, Tufts University

Enantioselectivity is the quintessential form of structure-sensitive surface chemistry, as differences in reactivity arise solely from the lack of mirror symmetry of the surface. Studying enantioselectivity on chiral surfaces provides insight into the design of enantioselective heterogeneous catalysts, which are important in pharmaceutical, agrochemical, and other industries. To determine the optimum surface facet for a given chemical reaction, it is essential to study the reaction on a wide variety of surface facets. Given the serial nature of surface science experiments on single crystals, high-throughput methods to study multiple facets at the same time would circumvent this issue. We have designed surface structure spread single crystals (S4Cs) that expose a vast variety of different surface facets on a single sample. Interestingly, a large portion of these facets are also chiral and therefore the use of S4Cs is ideal for studying for enantioselective surface chemistry. Tartaric acid decomposition on chiral Cu surfaces is known to be highly enantiospecific. With spatially resolved X-ray photoelectron spectroscopy (XPS), we have previously investigated the

Wednesday Morning, November 6, 2024

decomposition of tartaric acid on a Cu(110) ± 14o S4C where surfaces vicinal to Cu(14,17,2)R&Swere found to be the most enantiospecific. We have now combined these XPS results with scanning tunneling microscopy (STM) imaging to unveil the atomic-scale origins of the highly enantiospecific decomposition of tartaric acid on chiral Cu surfaces. We found extensive enantiospecific surface restructuring of surfaces vicinal to Cu(110) leading to the formation of facets vicinal to Cu(14,17,2). This reconstruction of the surface depends on both the TA enantiomer and the chirality of the surface itself, and is therefore enantiospecific. These results provide valuable insight into the origins of structure sensitivity for enantioselective reactions and demonstrate the efficacy of S4Cs in performing high-throughput surface science investigations.

9:45am **SS+2D+AMS-WeM-8 Competition between Hydrogen Bonding and van der Waals Interactions During Binary Self-Assembled Monolayer Formation**, *Rachael Farber, L. Penland, H. Hirushan, N. Dissanayake*, University of Kansas

Binary self-assembled monolayers (SAMs) comprised of polar and nonpolar molecules, such as 3-Mercaptopropionic Acid (MPA) and 1-Decanethiol (DT), offer the ability to carefully tune the interfacial properties of Au surfaces. The formation of molecularly precise binary SAMs through the displacement of one molecule with another *via* solution phase processing requires fine control over the structure and composition of the initial SAM. While DT has been extensively characterized using ultra-high vacuum (UHV) surface science techniques, the structural properties of MPA SAMs are less well understood. The relationship between solution phase processing procedures of MPA and island vacancy density, domain size, film uniformity, and the subsequent displacement behavior when exposed to DT, has not been established.

In this work, the effects of solution phase incubation temperature and time on MPA SAM formation and subsequent DT displacement behavior were determined using UHV scanning tunneling microscopy. Three MPA incubation procedures were studied: 3 hr MPA incubation at 35 °C (**MPA-1**), 3 hr MPA incubation at 25 °C (**MPA-2**), and 24 hr MPA incubation at 25 °C (**MPA-3**). While **MPA-1** and **MPA-2** both showed the characteristic MPA lattice, **MPA-1** had fewer domain boundaries and vacancy islands compared to **MPA-2**. **MPA-3**, which had the fewest domain boundaries and vacancy islands, showed regions of an MPA bilayer species across the surface. To determine the consequences of defect density and the presence of an MPA bilayer on DT displacement, **MPA-1**, **MPA-2**, and **MPA-3** were subsequently placed in a 2 µM DT solution for 20 min, 60 min, 3 hr, and 24 hr. **MPA-1** and **MPA-2** had comparable rates of DT displacement, with the formation of a high-density DT film across the surface within 3 hr. **MPA-3** had markedly slower DT displacement. Following a 24 hr incubation of **MPA-3** in the DT solution, small regions of the low-coverage, lying down phase (β) and 2-D gas phase (α) of DT were found across the surface. Only after a 48 hr incubation of **MPA-3** in DT did the high-density DT phase form. These results highlight the significance of the bonding interactions of the initial SAM on displacement kinetics during the formation of binary SAMs.

11:00am **SS+2D+AMS-WeM-13 Learning More with Less: High-Throughput Screening of Molecular Layer Deposition Processes**, *David Bergsman*, University of Washington **INVITED**

Because of its ability to deposit organic, inorganic, and hybrid ultrathin films with sub-nanometer thickness and compositional control, molecular layer deposition (MLD) has seen growing interest for use in technologies where precise interfacial control is essential, such as in semiconductor processing, membrane separations, and catalysis. However, development of these technologies is inhibited by the relatively slow process times for MLD vs atomic layer deposition and the large number of combinations of inorganic & organic reactants available to MLD.

This presentation will highlight the intrinsic advantages of accelerating MLD process development, both for technology development and for fundamental research. First, previous work in MLD process development will be highlighted, focusing on areas where comparisons between processes yielded fundamental insight into film growth phenomena. Then, an approach for rapidly screening new materials deposited by MLD using a custom-built, high-throughput, multiplexing MLD-style reactor will be discussed. In such a system, multiple reaction chambers are connected to shared reactants and pumping lines, allowing for the elimination of redundant reactor components and reducing capital costs compared to an equivalent number of independent systems. Finally, an example of how this approach can be applied to future technologies, such as EUV photolithography, will be given, demonstrating how materials made using

these parallel systems can be screened for their properties of interest and be used to obtain process-structure-property relationships.

11:30am **SS+2D+AMS-WeM-15 Organic Molecular Architectures Synthesized on Si(001) by Means of Selective Click Reactions**, *T. Glaser, J. Peters, Justus Liebig University Giessen, Germany; D. Scharf, U. Koert, Philipps University Marburg, Germany; Michael Dürr, Justus Liebig University Giessen, Germany*

The concept of molecular layer deposition on solid surfaces is promising for the synthesis of layers with well-controlled physical and physicochemical properties. Molecules with two functional groups are suitable building blocks for covalent layer-by-layer synthesis. However, with symmetric bifunctional organic molecules, i.e., with two identical functional groups at one molecule, side reactions which hinder the well-controlled layer-by-layer growth, e.g., by chain termination, may occur.

Here we solve this problem using a combination of two selective and orthogonal click reactions for controlled covalent layer-by-layer growth on Si(001). In order to do so, we combine ultrahigh-vacuum- (UHV)-based functionalization of the Si(001) surface with solution-based click chemistry for the attachment of the further layers. The starting point is the Si(001) substrate which is functionalized via selective adsorption of the bifunctional ethynylcyclopropylcyclooctyne (ECCO) molecule under UHV conditions [1]. This first-layer sample is then transferred into solution [2] in order to perform the subsequent layer-by-layer synthesis using the two orthogonal click chemistry reaction steps in an alternating fashion: First, a diazide is coupled in acetonitrile via a copper-catalyzed azide-alkyne click reaction; second, a layer of ECCO molecules is coupled via a catalyst-free, strain-promoted azide-alkyne click reaction. Without contact to ambient conditions, the samples are analyzed by means of X-ray photoelectron spectroscopy in UHV after each reaction step in solution; the N 1s spectra clearly indicated in the first step the selective click reaction of the primary azido group of the diazide molecule, whereas the tertiary azido group stayed intact. In the second step, this tertiary azido group was reacted selectively with the strained triple bond of the ECCO molecule in solution, forming a third layer of organic molecules on Si(001) with the terminal triple bond of ECCO available for further reactions according to this cyclic reaction scheme. Alternating application of the two orthogonal reaction steps then led to a well-controlled layer-by-layer growth up to 11 layers [3]; it opens the possibility for the controlled synthesis of layers with physical or physicochemical properties that alternate on the molecular scale.

[1] C. Länger, J. Heep, P. Nikodemiak, T. Bohamud, P. Kirsten, U. Höfer, U. Koert, and M. Dürr, *J. Phys.: Condens. Matter* 31, 34001 (2019).

[2] T. Glaser, J. Meinecke, C. Länger, J. Heep, U. Koert, and M. Dürr, *J. Phys. Chem. C* 125, 4021 (2021).

[3] T. Glaser, J. A. Peters, D. Scharf, U. Koert, and M. Dürr, *Chem. Mater.* 36, 561 (2024).

11:45am **SS+2D+AMS-WeM-16 Confinement Effects at Surfaces**, *J. Anibal Boscoboinik*, Brookhaven National Laboratory

Nanosized spaces at surfaces offer an interesting playground to understand the effect of confinement in chemistry and physics. Two examples will be described in this talk. In the first one, the water formation from hydrogen and oxygen is studied on a metal surface both in its bare state and also covered with a two-dimensional porous silicate. A change in reaction pathway is observed due to confinement effects. In the second example, nanosized silicate cages supported on a metal are shown to trap single atoms of noble gases through a new ionization-facilitated trapping mechanism. In this case, the gas phase species are first ionized. These ions can then enter the nanocages, at which point they get neutralized by an electron donated by the adjacent metal, resulting a neutral species that are kinetically trapped inside the confined space.

12:00pm **SS+2D+AMS-WeM-17 Facilitating CO₂ Capture Enabled by Weak Intermolecular Interactions Among CO₂, Water and PEEK-Ionene Membrane**, *Jennifer Yao, L. Strange, J. Dhas, PNNL; S. Ravula, J. Bara, University of Alabama; D. Heldebrant, Z. Zhu, PNNL*

Poly (ether ether ketone) (PEEK)-ionene membranes have shown significant potential for direct CO₂ capture due to their high selectivity, durability, and efficiency.¹ Despite their promise, the mechanisms of CO₂ transport through these membranes and the impact of water vapor on its CO₂ capture and diffusion remain poorly understood. Time-of-flight secondary ion mass spectrometry (ToF-SIMS) can detect and distinguish the characteristic molecular ions,^{2, 3} making it an ideal tool for studying complex intermolecular interactions of the CO₂, water and the membrane. In this study, a combination of isotopic labeling and SIMS provides a unique

Wednesday Morning, November 6, 2024

method to track small molecules in organic matrixes at nanoscale. We investigated the interactions of PEEK-ionene membranes with $^{13}\text{CO}_2$ and D_2O using cryo ToF-SIMS. ToF-SIMS 3D imaging provided chemical mapping of the distribution of these species from the surface down to several micrometers into the membrane. The cryo ToF-SIMS data did not show any significant enhancement of the $^{13}\text{C}/^{12}\text{C}$ ratio, implying weak CO_2 -membrane interactions and CO_2 vaporization even at $-130\text{ }^\circ\text{C}$ in vacuum condition. In contrast, cryo ToF-SIMS revealed a relatively uniform distribution of D_2O within the heavy water-loaded membrane. This suggests that water-membrane interactions are stronger than CO_2 -membrane interactions. Additionally, the presence of D_2O in the membrane did not enhance $^{13}\text{CO}_2$ retention, indicating weak CO_2 - D_2O interactions and minimal impact of water vapor on CO_2 diffusion within membrane. For comparison, ToF-SIMS data demonstrated that $^{13}\text{CO}_2$ readily reacts with a basic Na_2CO_3 solution to form $\text{NaH}^{13}\text{CO}_3$, highlighting the potential for modifying CO_2 -membrane interactions via functional group modifications. Specifically, introducing basic functional groups may enhance CO_2 -membrane interactions, whereas acidic modifications may reduce them.

References:

1. K. O'Harra, I. Kammakakam, P. Shinde, C. Giri, Y. Tuan, E. M. Jackson and J. E. Bara, ACS Applied Polymer Materials, 2022, 4, 8365-8376.
2. L. E. Strange, S. Ravula, Z. Zhu, J. E. Bara, P. Chen, D. J. Heldebrant and J. Yao, Surface Science Spectra, 2024, 31.
3. L. E. Strange, D. J. Heldebrant, S. Ravula, P. Chen, Z. Zhu, J. E. Bara and J. Yao, Surface Science Spectra, 2024, 31.

Wednesday Afternoon, November 6, 2024

Advanced Microscopy and Spectroscopy to Explore Field-Assisted Chemistry

Room 116 - Session AMS1-WeA

Advanced Microscopy and Spectroscopy to Explore Field-Assisted Chemistry I

Moderators: Sten Lambeets, Pacific Northwest National Laboratory, Daniel E Perea, Pacific Northwest National Laboratory

2:15pm **AMS1-WeA-1 Influence of External Electric Fields on Catalytic Reactions: An Insight through Atom Probe Microscopy and Field Ion Microscopy**, *Thierry Visart de Bocarmé*, Université libre de Bruxelles, Belgium **INVITED**

The study of catalytic reactions under the influence of external electric fields has emerged as a significant area of research in the field of chemistry. This research is driven by the potential to manipulate reaction pathways and enhance catalytic efficiency. This presentation will delve deeper into the role of Atom Probe Microscopy (APM) and Field Ion Microscopy (FIM) in elucidating these effects.

Commercial APM models, with their unique abilities to provide 3D atomic-scale compositional information, enable to probe the catalyst's structure and composition before or after reaction but hardly *during* reaction. Using an isolated counter electrode with a tunable static potential, the static field on the catalyst can be adjusted to the desired value by convenient choices of the respective voltages on the sample and the counter electrode. Short voltage pulses are then superimposed on the static voltage of the counter electrode to raise the electric field at the sample surface to trigger field desorption or field evaporation. This methodology aids in measuring how electric fields modify the catalyst's surface composition during the ongoing reaction, and provides insights on the reaction pathways.

On the other hand, FIM, with its capacity for direct imaging of individual atoms and even surface reactions in real-time, provides an unparalleled view of the instant state of the catalyst surface, i.e. the extremity of a sharp tip the size and shape of which approximate those of one single catalytic grain. This enables to directly visualize how electric fields of some 10 V.nm^{-1} affect the behavior of reactants and products on the catalyst surface, thereby influencing the catalytic reactions.

The presentation will highlight several case studies where APM and FIM have been used in providing insights into the influence of electric fields on catalytic reactions. The hydrogen-oxygen reaction on rhodium surfaces has been monitored by video FIM and probed using voltage pulses. The results show that, on one single catalytic grain, the reaction can proceed simultaneously through Langmuir Hinshelwood and Mars Van Krevelen-type mechanisms. The water-gas shift reaction on gold surfaces at room temperature has been investigated by FIM and APM and shows that the reaction proceeds through the formation of a hydroxyl-type surface intermediate that is reacted off by the presence of CO gas. Eventually, the nitrogen oxide adsorption on platinum surfaces and its field-dependance will be discussed.

2:45pm **AMS1-WeA-3 Charged Surfaces Theory, Atom Probe Microscopy and Other High-Field Techniques Relevant to Electric-Field-Assisted Chemistry**, *Richard Forbes*, University of Surrey, UK **INVITED**

The action of high electrostatic (ES) fields on chemical reactions is different in solution and in near vacuum, is different depending on whether the chemical entity of interest is in free space or adsorbed onto a substrate surface, and may depend on the nature of the substrate. This talk focuses primarily on the case of adsorption on metals, in a vacuum environment. It seeks to explore/clarify how (and to what extent) high ES-field experimental techniques might be used to investigate the related high-field surface chemistry.

A substantial introduction to necessary background knowledge will include high-level summaries of: (a) charged-surfaces theory at various model-levels, from classical conductor to density-functional theory approaches; (b) basic scientific concepts related to the techniques of interest; (c) the science of how the techniques work, including: field adsorption, field ionization, operating-gas dynamics, field evaporation, field desorption, and basic electrohydrodynamics; and (d) our rather limited knowledge of practical high-ES-field surface chemistry. One possibility is so-called electrocatalysis. Thus, the hypothesis of Lambeetz and colleagues is that the ES field might enhance the rate of a catalytic reaction, in particular

hydrogenation of simple carbon-based molecules on a transition-metal substrate.

The techniques of primary interest are field ion microscopy, field desorption mass spectroscopy, and atom-probe tomography (APT), with some emphasis on the last of these. In some respects, APT is the most sensitive of these techniques, but it also seems that for some or many applications there might be signal-level issues and that further technical development of the technique might be needed/helpful.

A question that probably needs a clearer answer is the following: precisely what information about electric-field-assisted chemistry do we wish to get out of the use of these techniques (or precisely what questions do we wish to answer)? And what can we actually hope to achieve in practice?

The talk aims to include references to further information. A copy of the slides and references will be mounted on ResearchGate (search "Richard G Forbes") some weeks after the AVS meeting.

3:15pm **AMS1-WeA-5 Ab-Initio Simulation of Field Evaporation in Atom Probe Tomography**, *Wolfgang Windl*, The Ohio State University; *J. Qi*, Ohio State University; *E. Marquis*, University of Michigan **INVITED**

Atom probe tomography (APT) is a three-dimensional characterization technique that ideally can resolve both positions and chemical identities of the atoms in a material. Unlike "focused-beam" microscopy techniques which rely on X-rays or electron beams for imaging, in APT, atoms in the sample are imaged by themselves. Individual atoms or molecules are field-evaporated from the surface of a needle-shape specimen under an intense electric field and fly towards a two-dimensional detector where their impact positions and sequence are recorded. From that, along with the chemical identities revealed by a mass spectrometer, a three-dimensional distribution of the atoms in the specimen can be reconstructed. However, since field evaporation is a destructive process, it is impossible to verify reconstruction results and quantify uncertainties in experiments. In this case, atomic-scale forward modeling becomes the only viable way to produce verifiable virtual data to test reconstruction where each single atom is traceable. A number of atomic modeling approaches have been developed during the past 25 years, however, all of them are implicitly based on harmonic transition state theory which can only predict the rate of transition from one state to another but not describe any dynamics between the two states. As an alternative, we propose to simulate field evaporation with full dynamics using molecular dynamics (MD) simulations. For that, we have integrated field evaporation events as part of the MD simulation by combining the electrostatics from the finite element field evaporation code TAPSim with the MD simulator LAMMPS. With full dynamics, atoms in the specimen are evaporated in an "ab-initio" way as a result of the competition between the interatomic forces and the electrostatic forces. To demonstrate our full-dynamics approach, we will show results that explain for the first time the enhanced zone lines in field evaporation maps, "ab-initio" prediction of the evaporation sequence in [001]-oriented γ -TiAl intermetallic compounds explaining the observed artifact of mixed layers, and simulations of GP-zones in Al-Cu alloys that demonstrate the inherent inaccuracies in resolving atomic positions. The overarching goal of this work is to guide APT reconstruction using our "ab-initio" simulation data, gain better interpretations of fundamental processes, and take the quantification capability of the APT technique to the next level.

Advanced Microscopy and Spectroscopy to Explore Field-Assisted Chemistry

Room 116 - Session AMS2-WeA

Advanced Microscopy and Spectroscopy to Explore Field-Assisted Chemistry II

Moderators: Sten Lambeets, Pacific Northwest National Laboratory, Daniel E Perea, Pacific Northwest National Laboratory

4:15pm **AMS2-WeA-9 Lanthanide Adsorption in Micras: The Implications for Rare Earth Elements Separations**, *Y. Wen*, US DOE Ames National Laboratory; *K. Verma*, Ames National Laboratory; *D. Jing*, Iowa State University; *M. Lacount*, *S. Kathmann*, Pacific Northwest National Laboratory; *Tanya Prozorov*, US DOE Ames Laboratory **INVITED**

Rare earth elements (REEs) are critical to the economic growth and national security of the United States, but their supply chain is vulnerable to disruptions. To harness underutilized sources of REEs, it is important to understand the localized environments in which these elements occur.

Wednesday Afternoon, November 6, 2024

Regolith-hosted ion-adsorption clays selectively absorb heavy REEs (HREEs) released through the weathering and dissolution of granites and other igneous rocks by rainwater. This REE adsorption trend is recognized, yet the adsorption mechanisms remain poorly understood.

Our results show that micas, which are structurally and chemically similar phyllosilicates, exhibit a different pattern of REE adsorption. Notably, micas adsorb Nd (a light REE) more readily than Yb (a heavy REE), deviating from the HREE adsorption trend in regolith-hosted clays. Our findings further revealed the colocalization of lanthanides with impurity ions within the mica structures, underscoring the significant role of internal electric potentials in influencing REE adsorption. This unusual adsorption behavior in micas due to the electric potentials within their structure provides crucial experimental evidence that impurities can be used to tune REE adsorption and separation in layered materials.

We employ scanning transmission electron microscopy in combination with analytical spectroscopy and electron holography experiments for detailed spatio-chemical analysis of micas exposed to aqueous solutions containing Nd and Yb. We monitor the d-spacing of minerals, using it as a single electron beam-damage indicator throughout our imaging and spectral analysis processes. Atom Probe Tomography (APT), X-ray Photoelectron Spectroscopy (XPS) and computational modeling in combination to deepen our understanding of the fundamental factors that govern REE adsorption in micas. These insights are instrumental in guiding the development of novel geo-inspired materials for the effective separation of rare earth elements from diverse feedstocks.

4:45pm AMS2-WeA-11 Single-Molecule Spectroscopic Probing of N-Heterocyclic Carbenes on a Two-Dimensional Metal, Nan Jiang, University of Illinois Chicago

N-heterocyclic carbenes (NHCs) have recently proven to be powerful ligands for planar surface modification due to their remarkable structural diversity, property tunability, and high affinity to a diverse array of elements. However, the utilization of NHCs for planar surface modification has almost exclusively been limited to bulk substrates; the exploration of NHC modification of two-dimensional (2D) materials remains largely uncharted despite its promise for wide energy and electronic applications. Here we investigate the adsorption of NHCs on a 2D metal, specifically monolayer boron (i.e., borophene), at the single-molecule level using tip-enhanced Raman spectroscopy, scanning tunneling microscopy/spectroscopy (STM/S), and density functional theory calculations. Single-molecule optical spectroscopy reveals the distinct interfacial interactions between individual NHCs and borophene, in covalent (boron-carbon bonding) and van der Waals-type manners, highlighting the role of steric effects in determining the binding mode. Furthermore, the impact of NHC adsorption on borophene's electronic properties is demonstrated by local work function reductions, as measured quantitatively by single-molecule STS. In addition to providing novel insight into NHC-substrate interactions in the 2D regime, this study opens up an avenue for single-molecule studies of NHC chemistry, promising to promote advances in understanding and inform ongoing efforts to devise and realize new NHC-related applications.

5:00pm AMS2-WeA-12 Electric Fields and CO₂ Coverage Effects on the Surface Chemistry of La-Based Perovskites, Ariel Whitten, J. McEwen, Washington State University; **E. Nikolla,** University of Michigan, Ann Arbor; **R. Denecke,** Leipzig University, Germany

Perovskite-based materials are more stable than metal anode catalysts in electrochemical CO₂ reduction processes, but perovskites have reduced activity as compared to metal catalysts such as Ni. For perovskites to be an alternative catalyst for this process, the perovskite surface needs additional augmentations to increase the activity such as the introduction of active sites like oxygen vacancies or external influences like electric fields. We propose using La-based perovskites (LaNiO₃, LaCoO₃ and LaFeO₃) which are known to be highly active in CO₂ reduction and investigate these surfaces using both experimental and first principles-based calculations. In a previous project, we deconvoluted XPS spectra of LaNiO₃ and LaCoO₃ finding that the higher energy peak in the O 1s spectra occurred in large part to the adsorption of water but other adspecies (H, O, OH and CO₂) gave smaller contributions to the peak. Although understanding the surface science of co-electrolysis with H₂O and CO₂ is the ultimate goal of the project, the adsorption and conversion of CO₂ are a widely acknowledged barrier to CO₂ reduction. Therefore, studying the nature of CO₂ interactions with the surface is imperative to building on the critical knowledge needed to improve this process. From our initial results studying CO₂ adsorption at differing coverages (Figure 1), we find that interactions calculated using the

lattice gas method between adspecies travel mainly through the surface (Figure 2) and cause a surface rearrangement depending on adsorbate configuration, adsorption strength and B-site material. This indicates the limiting factor of CO₂ adsorption is the concentration of charge in the surface that is necessary to stabilize the adspecies. The stabilization of adsorbates can therefore be improved by adding charge via external electric fields. Our studies of electric fields on clean surfaces indicate that increased electric fields lead to a drastic fluctuation in the plane averaged local potential, which can decrease the stability of the surface. Thus, the strength of the electric field needs to be calibrated so that it adds charge to the surface without causing its decomposition. Moreover, the formation of surface oxygen vacancies is spontaneous under negative electric fields on LaFeO₃. Thus, the perovskite anode of an electrochemical cell will form active sites that spontaneously increase its activity. In further studies, we aim to understand the effects of coverage on the adsorption of CO₂ using nudged elastic band calculations and an effect of electric fields has on the adsorption and activation of CO₂.

5:15pm AMS2-WeA-13 Interfacial Quantum Electric Fields, Shawn Kathmann, Pacific Northwest National Laboratory

Electric fields and voltages within and at the interfaces of matter are relevant to catalysis, crystallization, materials science, biology, and aqueous chemistry. Accurate measurements of fields and voltages of matter has been achieved using electron holography/tomography (EHT) and can be directly compared with quantum mechanical calculations. From these findings all interfaces have large intrinsic local electric fields (~ 10 GV/m = 1 V/Å) and voltages even if these materials are macroscopically electrically neutral. The use of very weak applied fields ($<10^{-3}$ V/Å) causes materials to respond, changing both the magnitude and spatial distribution of the intrinsic electric fields. The resulting interfacial response fields, i.e., $E_{\text{resp}}(r) = E_{\text{intr}}(r) + E_{\text{appl}}(r)$, have been measured using EHT and are similarly large as the intrinsic fields even though the applied field is very weak. These large fields can and do alter adsorbed species electronic states (e.g., bonding/antibonding orbitals, luminescence, chemical reaction barriers, electron transfer, etc.) as well as rotational and vibrational states. When characterizing fields and voltages in matter, it is essential to specify exactly where they are being evaluated and over what spatial regions of the quantum charge density do different measurements probe (e.g., electron holography tomography vs. vibrational Stark spectroscopies). Here we outline the chemical physics, quantum, and statistical mechanics relevant to these findings and their consequences on how we understand, control, and exploit interfacial fields.

This work is sponsored by the U.S. Department of Energy, Office of Basic Energy Sciences, Division of Chemical Science, Geosciences, and Biosciences Condensed Phase and Interfacial Molecular Sciences Program. Pacific Northwest National Laboratory (PNNL) is a multiprogram national laboratory operated for DOE by Battelle.

Surface Science

Room 120 - Session SS+2D+AMS-WeA

Defects Nanoarchitecture and Complex Systems

Moderators: Dario Stacchiola, Brookhaven National Laboratory, **Zhenrong Zhang,** Baylor University

2:15pm SS+2D+AMS-WeA-1 Exploring ZIF-8 Vibrational Spectra with Its IR Peak Assignments and Defect Signal Characterization, Mueed Ahmad, Stony Brook University/Brookhaven National Laboratory; **R. Patel,** University of Minnesota; **D. T. Lee,** Stony Brook University/Brookhaven National Laboratory; **P. Corkery, A. Kraetz,** Johns Hopkins University; **P. Prerna,** University of Minnesota; **S. Tenney, D. Nykpanchuk, X. Tong,** Brookhaven National Laboratory; **J. Siepmann,** University of Minnesota; **M. Tsapatsis,** Johns Hopkins University; **J. Boscoboinik,** Stony Brook University/Brookhaven National Laboratory

Surface chemistry is critical in elucidating the functional properties of Zeolitic Imidazolate Framework-8 (ZIF-8), a versatile material with applications in gas separation, sensing, catalysis, and lithography. Comprising zinc that is tetrahedrally coordinated with 2-methylimidazolate (2mIm) linker, ZIF-8 is synthesized through various methodologies to modulate its crystalline characteristics and integration into nanocomposites including powder, film and membranes.

Despite efforts to achieve defect-free ZIF-8 structures, deviations in structure may occur due to the presence of defects such as vacancies in 2mIm ligands, zinc vacancies, and physically adsorbed 2mIm molecules

Wednesday Afternoon, November 6, 2024

within pores, substantially impacting its performance and stability. Infrared reflection absorption (IRRA) spectroscopy is employed to probe these defects, although interpretations of IR spectra vary across studies. Our investigation employs experimental IR spectroscopy alongside first-principles molecular dynamics (FPMD) simulations to scrutinize ZIF-8's vibrational spectra, with a specific focus on defect-induced signals. X-ray Photoelectron Spectroscopy (XPS) is utilized to probe the surface composition of the material up to a depth of 10 nanometers.

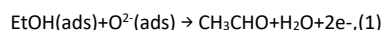
We have highlighted the prevalence of defects in the synthesis of ZIF-8 films/membranes, which are critical in gas separation applications. Notably, we observed the formation of SiO_x as a notable defect, stemming from exposure to silicon grease in vacuum reactors. This phenomenon is pertinent to materials synthesized under vacuum conditions, as vacuum grease residues may persist over time.

Through the resolution of conflicting interpretations of IR spectra and the identification of defect signals, our objective is to gain a comprehensive understanding to enhance the quality control and design of ZIF-8-based materials for diverse applications.

2:30pm SS+2D+AMS-WeA-2 Molecular Sensing ZnO Surfaces Studied by Operando Low-Energy Ion Beam Analysis, Taku Suzuki, Y. Adachi, T. Ogaki, I. Sakaguchi, National Institute for Materials Science, Japan

1. Introduction

The basic mechanism of the resistive gas sensing has been established; it is essentially a redox reaction of the surface mediated by the negatively charged oxygen adsorbate. For example, the sensing of ethanol (EtOH) with the ionosorbed oxygen of O²⁻ is written as,



where (ads) denotes an adsorbate. It is reasonable to assume that the gas sensing properties differ between crystallographic atomic planes. Indeed, the crystal plane dependent gas sensing response has been studied by many research groups in the last decade for EtOH sensing by ZnO, which is one of the most intensively studied target gas – sensing material combinations. The specific knowledge of the crystal plane dependence of gas sensing is useful for the development of sensing materials.

The ZnO crystal plane dependence of the gas sensing properties has typically been studied using a nanocrystal. However, the effect resulting from the contact between the particles has hindered straightforward interpretation. To overcome this problem, the ZnO crystal plane dependence of the EtOH sensing was investigated using an analytical approach in the present study, namely low-energy ion scattering spectroscopy (LEIS) combined with the pulsed jet technique.

2. Method: LEIS combined with pulsed jet

We applied a newly developed He⁺ LEIS combined with the pulsed jet technique to analyze the surface structure of ZnO during the EtOH sensing. In this novel technique, the free gas jet is periodically blown onto the sample surface to simulate the gas sensing surface in a vacuum as one under the realistic working condition, while the background pressure is kept low enough for the operation of He⁺ LEIS.

The sample was ZnO single crystals with an atomically flat mirror-polished surface. Four dominant low-index surfaces, which are Zn-terminated (0001) (c+), O-terminated (0001) (c-), (10-10) (m), and (11-20) (a), were used to evaluate the crystal orientation dependent gas sensing properties.

References

- [1] N. Saito et al., Chemical Sensors 39(2023)108. (Japanese)
- [2] T. Suzuki et al., Surfaces and Interfaces 35(2022)102371.
- [3] T. Suzuki et al., Appl.Surf.Sci.538(2021)148102.

2:45pm SS+2D+AMS-WeA-3 Finding Surface Defects in Electronic Materials, Sujitra Pookpanratana, National Institute of Standards and Technology

INVITED

All electronic materials contain a wide range of defects ranging in length scales from point defects to micrometer (or sub-millimeter) scale features. Some defects can be beneficial, benign, or detrimental to the functionality of the material. It's critical to identify and locate defects, and determine their impact in the host material. Here, I will highlight the identification of defects and their impact in 2D graphene-based systems and wide bandgap semiconductors using photoemission electron microscopy (PEEM). PEEM is a nanoscale, surface-sensitive, full-field imaging technique based on the photoelectric effect. PEEM provides real space imaging of surfaces with enhanced contrast mechanism based on topographic and electronic properties, and measurement of electronic properties. In the first example,

we image epitaxial graphene (EG) topography in real space and measure the electronic structure of monolayer EG regions with micrometer-scale angle resolved photoemission (μ -ARPES). We detect characteristic electronic features of graphene such as the Dirac points and the π -band, and the electronic flat band at region with different contrast [1]. Through Raman spectroscopy on the same regions that were analyzed by PEEM, and we estimated a significant amount of compressive strain ($\sim 1.2\%$) coinciding with the flat band region [1]. In the second example, we highlight the full-field PEEM capability by following the de- and re-intercalation of 2D Ag within EG under heating conditions. For the 2D Ag system, we find Ag clusters initially diffuse to the top EG surface and finally re-intercalate through defects with the Ag intercalation front to be $0.5 \text{ nm s}^{-1} \pm 0.2 \text{ nm s}^{-1}$ [2]. The EG defects serve as intercalation "doors." Lastly, we will show extended surface defects propagating through epitaxy GaN and β -Ga₂O₃ which also induce the presence of bandgap states.

[1] F. Niefind, H. G. Bell, T. Mai, A. W. Hight Walker, R. E. Elmquist, S. Pookpanratana, J. Appl. Phys. 131, 015303 (2022).

[2] F. Niefind, Q. Mao, N. Nayir, M. Kowalik, J. J. Ahn, A. Winchester, C. Dong, R. A. Maniyara, J. Robinson, A. van Duin, and S. Pookpanratana, Small 20, 2306554 (2024).

3:15pm SS+2D+AMS-WeA-5 SSD Morton S. Traum Award Finalist Talk: Silver Iodide – Surface Structure and Ice Nucleation Investigated by Noncontact AFM, Johanna Hütner¹, D. Kugler, Vienna University of Technology, Austria; F. Sabath, Bielefeld University, Germany; M. Schmid, Vienna University of Technology, Austria; A. Kühnle, Bielefeld University, Germany; U. Diebold, J. Balajka, Vienna University of Technology, Austria
Silver iodide (AgI) is used as a cloud seeding material due to its ability to nucleate ice efficiently, which is explained by the good lattice match between AgI and hexagonal ice. The basal (0001) cleavage plane of AgI deviates from the lattice of hexagonal ice by as little as 2.5%. However, AgI consists of stacked planes of positively charged Ag⁺ alternating with negatively charged I⁻. Cleaving a AgI crystal along the (0001) plane thus exposes Ag⁺ and I⁻ terminated surfaces. Both terminations are polar and inherently unstable.

We present atomically resolved noncontact atomic force microscopy (NC-AFM) images that show how AgI(0001) surfaces compensate for this non-zero electric dipole perpendicular to the surface. Both Ag and I terminated surfaces form reconstructions, whose structure affects their ice nucleating abilities. NC-AFM images of UHV cleaved surfaces exposed to water vapor reveal that ice forms an epitaxial layer only on the Ag terminated surface, whereas on the I termination ice forms three-dimensional clusters.

These atomic-level observations could enhance our understanding of ice formation processes in the atmosphere.

3:30pm SS+2D+AMS-WeA-6 SSD Morton S. Traum Award Finalist Talk: Reversible Non-Metal to Metal Transition and Effective Debye Temperatures of Highly Crystalline NiFe₂O₄ Thin Films, Arjun Subedi², D. Yang, X. Xu, P. Dowben, University of Nebraska-Lincoln, USA

The surface of NiFe₂O₄ thin film undergoes a conductivity change with temperature. X-ray photoelectron spectroscopy (XPS) of NiFe₂O₄ thin film at room temperature showed large binding energy shifts in Ni 2p_{3/2}, Fe 2p_{3/2}, and O 1s core levels, due to photovoltaic surface charging indicating that prepared NiFe₂O₄ thin film was dielectric or non-metallic at room temperature. The core level binding energy shifts, due to photovoltaic surface charging, were found to be around 5 eV for each of the core levels at room temperature. The core level binding energy shifts decreased when the thin film was annealed in vacuum. The XPS core level binding energy shifts from the expected values became negligible at an elevated temperature of 410 K and beyond. This suggests that NiFe₂O₄ thin film became metallic at the temperature of 410 K and beyond. When the sample cooled down to room temperature, the sample reversibly became more dielectric, showing again the same core level binding energy shifts of 5 eV. Such reversible phase change of the thin film was further supported by the reversible Fermi edge shift with temperature. Low energy electron diffraction (LEED) images, taken for the NiFe₂O₄ thin film surface, showed that the surface was highly crystalline throughout the reversible temperature controlled non-metal to metal transition. The XPS spectra of Ni 2p_{3/2}, Fe 2p_{3/2}, and O 1s core levels taken at different temperatures showed that the changes in core level binding energies followed a proposed Arrhenius-type model with temperature. The effective bulk Debye

¹ SSD Morton S. Traum Award Finalist

² SSD Morton S. Traum Award Finalist

Wednesday Afternoon, November 6, 2024

temperatures of 629.10 ± 58.22 K and 787.03 ± 52.81 K were estimated using temperature dependent intensities of Fe $2p_{3/2}$ and Ni $2p_{3/2}$ XPS spectra respectively indicative of different sites for Fe and Ni. The effective surface Debye temperature of 249.7 ± 11.1 K was estimated using temperature dependent intensities of LEED. Lower effective Debye temperature was observed for surface, as expected. The phase transition, the estimates of the effective Debye temperatures, and the model applied to the core level binding changes with temperature altogether shed light on the fundamental properties of the material with temperature.

4:15pm **SS+2D+AMS-WeA-9 In situ Structure Study of a MnOx-Na₂WO₄/SiO₂ Catalyst for OCM under Na₂WO₄ Melting Conditions**, **Yong Yang**, ShanghaiTech University, China; **D. Wang**, **E. Vovk**, ShanghaiTech.edu.cn, China; **Y. Liu**, **J. Lang**, ShanghaiTech University, China
MnO_x-Na₂WO₄/SiO₂ catalyst exhibited notable C₂ selectivity/yield in the oxidative coupling of methane (OCM), a promised green chemistry reaction^[1, 2]. Nevertheless, the reaction mechanism of this catalyst remains a subject of contention, particularly regarding the role of Na₂WO₄ in the activation^[3, 4]. In this study, *in situ* characterizations of a TiO₂-modified MnO_x-Na₂WO₄/SiO₂ catalyst, are conducted by XRD and XPS correlating to the OCM reaction condition, focusing on the simultaneous phase transition of catalyst components within its activation temperature zone. The online MS along with XPS/XRD coupled activity study confirm that transition from Mn³⁺ to Mn²⁺ stands as a pivotal factor influencing the reactivity. *In situ* XRD further revealed that in this narrow temperature window there is a particular three-step Na₂WO₄ phase change, ending as molten salt, right before the substantial Mn³⁺ to Mn²⁺ transfer initiated. In addition, the rarely observed Na₂WO₄ behavior as molten salt is obtained by *in situ* XPS with rapid spectra collected during an on-stage heating process. A sensitive self-reduction of the tungsten upon heating to melting point is found. These comprehensive *in situ* catalyst characterizations, covering the extensive structure-activity relationship from solid state to partial molten salt condition, providing a interlocking pathway for the reactive oxygen species transferring at high temperature. The results provides new important insight into the complex MnO_x-Na₂WO₄/SiO₂ catalyst as a key to understand the activation mechanism of NaWmSi catalyst in OCM.

[1] Lunsford JH, Catalytic conversion of methane to more useful chemicals and fuels: a challenge for the 21st century. *Catalysis today* 63 (2000) 165-174;

[2] Lunsford JH The Catalytic Oxidative Coupling of Methane. *Angewandte Chemie International Edition in English* 34 (1995) 970-980;

[3] Si J, Zhao G, Sun W, Liu J, Guan C, Yang Y, Shi XR, Lu Y Oxidative Coupling of Methane: Examining the Inactivity of the MnO_x-Na₂WO₄/SiO₂ Catalyst at Low Temperature. *Angewandte Chemie International Edition* 61 (2022) e202117201

[4] Fang X, Li S, Gu J, Yang D Preparation and characterization of W-Mn catalyst for oxidative coupling of methane. *J Mol Catal* 6 (1992) 255-261

4:30pm **SS+2D+AMS-WeA-10 Characterization of Nanoplastics Samples**, **T. Roorda**, **M. Brohet**, **S. Campos Jara**, **Irene Groot**, Leiden University, Netherlands

Plastic particles in the ocean have become a contaminant of emerging concern due to their damage to humans and marine animals. Of all plastic production, which is increasing still, it has been shown that more than 99% of plastic waste which ends up in the oceans cannot be accounted for. The belief is that all of this plastic degrades to a nano-sized scale which is extremely hard to detect. In order to understand the fate of nanoplastics in aquatic environments, we must have a better understanding of the degradation mechanisms at an atomic and chemical level. In this project, we have developed procedures to evaporate powdered materials and deposit them onto a prepared surface. The deposition of nanoplastics is confirmed by mass spectrometry, Auger electron spectroscopy, and X-ray photoelectron spectroscopy. Using atomic force microscopy combined with scanning tunneling microscopy, the deposited plastics are investigated.

We also investigate plastics samples after several degradation mechanisms, such as oxygenation, hydrogenation, UV exposure, and thermal annealing. After degradation, the plastics samples are studied in ultra-high vacuum with atomic force microscopy combined with scanning tunneling microscopy and with X-ray photoelectron spectroscopy.

4:45pm **SS+2D+AMS-WeA-11 Oxidation of NiCr and NiCrMo- Unraveling the Role of Mo with XPEEM Studies**, **Keithen Orson**, **D. Jessup**, University of Virginia; **W. Blades**, Juniata College; **J. Sadowski**, Brookhaven National Laboratory; **Y. Niu**, **A. Zakharov**, Lund University, Sweden; **P. Reinke**, University of Virginia

Nickel-chromium based superalloys combine good mechanical strength with excellent resistance to corrosion over a wide range of conditions. Passivity stems primarily from a thin layer of chromium oxides and hydroxides and increasing Cr content above a threshold of 11-15wt% results in a protective passive layer. Adding minor alloying elements like Mo has an outsized impact on corrosion resistance, but there is debate in literature over the mechanism of this action. To investigate the interplay of Cr concentration and Mo alloying, the early-stage oxidation (0-65 Langmuir of O₂) of Ni₂₂Cr, Ni₅Cr, and Ni₂₂Cr₆Mo were studied on a clean metal surface and moderate temperatures (450-500 °C). The oxidation was studied in-situ using x-ray photoelectron microscopy (XPEEM), which yields x-ray absorption hyperspectral images at 0, 5, 20, and 65 L of exposure, and a timeseries observing the oxide evolution from 0 to 65L at a single photon energy representative of Cr₂O₃. XPEEM valence band spectra, and conventional XPS study of the same samples complement the experiment. To analyze the ~10⁷ spectra produced by hyperspectral imaging, several data dimensionality reduction techniques including principal component analysis and non-negative matrix analysis were used to gain insight into the oxide evolution, the species present, and their spatial distribution. The amounts of each species present in the hyperspectral images were quantified using cosine similarity. Oxidation of Ni₂₂Cr produces islands of Cr₂O₃ along with a surface oxide, while on Ni₅Cr larger, sparser islands are observed. For both binary alloys the oxide grows in a layer-plus-island morphology. The oxide island chemistry of Ni₅Cr appears to include some NiO as well as Cr₂O₃. Ni₂₂Cr₆Mo, on the other hand, does not nucleate oxide islands visible with XPEEM but instead forms a continuous oxide layer whose thickness increases over time. This is commensurate with a layer-by-layer growth mode which is a significant advantage for protective function. This observation has implications for Mo's protective mechanism in the passive film, suggesting that Mo may be protecting from localized breakdown by altering the morphology of the oxide to produce a more uniformly protective oxide layer.

5:00pm **SS+2D+AMS-WeA-12 An Investigation of Local Distortions on High Entropy Alloy Surfaces**, **Lauren Kim**, University of Wyoming; **P. Sharma**, Lehigh University; **G. Balasubramanian**, Lehigh University; **T. Chien**, University of Wyoming

High entropy alloys (HEAs) are a widely studied family of materials that typically contain five or more elements. There are many combinations of elements that can create HEAs, and material properties can be tuned simply by changing elemental compositions. These properties of HEAs result in numerous applications, such as catalysis, energy storage, and aerospace engineering refractory materials. Severe-lattice-distortion is identified as one of the four core effects impacting the physical properties in HEAs. In this work, we demonstrate atomic resolution images of the surface of a CrMnFeCoNi HEA (Cantor alloy) using scanning tunneling microscopy (STM). This data allows us to determine lattice local distortions unambiguously. Additionally, we report our findings on the types of local defects on the surface, such as grain boundaries, phase changes, and amorphization, and how these defects can impact local distortions of the crystals nearby.

5:15pm **SS+2D+AMS-WeA-13 Grain Boundary and Twin Boundary Solute Segregations in Nanocrystalline Al-Mg Alloy**, **Xuanyu Sheng**, **z. Shang**, **A. Shang**, Purdue University, China; **H. Wang**, **X. Zhang**, Purdue University

Chemical segregations at grain boundaries (GBs) have been broadly investigated in Al alloys. However, there are limited experimental evidence demonstrating the dependence of solute segregation on GB characteristics. Here, we quantified solute segregation at GBs in nanocrystalline Al-1Mg (at.%) alloy by combining energy-dispersive X-ray spectroscopy, high-resolution scanning transmission electron microscopy and automated crystallographic indexing and orientation mapping. The dependence of solute segregation on the grain boundary misorientation angle is analyzed. Due to their higher excess free volume, high angle grain boundaries contain more Mg solutes than the low angle grain boundaries. Furthermore, coherent twin boundaries (CTBs) exhibit low solute segregation. However, incoherent twin boundaries (ITBs) display greater solute concentration. The different solute segregation behavior between CTBs and ITBs originates from their grain boundary structure. The solute segregation behavior reported here may shed light on the GB engineering of Al alloys.

Wednesday Afternoon, November 6, 2024

5:30pm **SS+2D+AMS-WeA-14 Charge Ordering Phase Transition in Bilayer Sn on Si(111)**, *Nathan Guisinger*, *M. Chan*, Argonne National Laboratory; *C. Lilley*, University of Illinois - Chicago

The atomic-scale investigation of the “bilayer” reconstruction of Sn on heavily doped n-type Si(111) was performed with scanning tunneling microscopy. When cooled to 55K, the bilayer reconstruction undergoes both a structural and electronic transition. Structurally, the dimer units of the bilayer shift to form a herringbone pattern with a rhombohedral ordering. The electronic structure transitions into a very uniform square lattice with similar dimensions to the structural dimers. There are distinct differences between the structural and electronic spacing that resolves itself when counting multiple periods. This ordering is like behavior observed in materials that exhibit charge density waves. Furthermore, STS point spectra show a transition from a small gap to a large insulating gap at low temperature that is consistent with a transition to a Mott insulating ground state. The charge ordering coupled with the relaxation to a Mott insulating phase upon cooling the Sn bilayer presents unique physics when the dimensionality is reduced from the bulk.

5:45pm **SS+2D+AMS-WeA-15 SSD Morton S. Traum Award Finalist Talk: On-Surface Design of Highly-Ordered Two-Dimensional Networks Stabilized by Nonmetal Atoms**, *Alisson Ceccatto*¹, University of Campinas (UNICAMP), Brazil; *G. Campi*, Yachay Tech University, Ecuador; *V. Carreño*, *E. Ferreira*, University of Campinas (UNICAMP), Brazil; *N. Waleska-Wellenhofer*, *E. Freiburger*, *S. Jaekel*, Friedrich-Alexander-University Erlangen-Nürnberg (FAU), Germany; *C. Papp*, Freie Universität Berlin, Germany; *H. Steinrück*, Friedrich-Alexander-University Erlangen-Nürnberg (FAU), Germany; *D. Mowbray*, Yachay Tech University, Ecuador; *A. de Siervo*, University of Campinas (UNICAMP), Brazil

Supramolecular nanoarchitectures have been widely explored to precisely design low-dimensional materials at atomic and molecular levels [1]. Such control is mainly based on bottom-up fabrication methods, e.g. on-surface synthesis, by combining molecular building blocks and atoms to engineer novel nanomaterials [2]. Particularly, the self-assembled monolayers (SAMs) of organic molecules present the potential for applications in nanoelectronics due to their reversible non-covalent interactions [3]. Such intermolecular interactions allow the fabrication of almost defect-free supramolecular nanostructures. Typically, the geometry of these nanoarchitectures can be controlled by the insertion of metal and non-metal atoms in the reaction process. To date, the adatom-mediated SAM fabrication concentrates on the use of metal adatoms, especially d metals (Cu, Co, Au, and Fe) [4]. Herein, by combining scanning tunneling microscopy (STM) measurements and density functional theory (DFT) calculations, we report the 2D self-assembled of 1,3,5-tris[4-(pyridin-4-yl)-[1,1'-biphenyl]]benzene (TPyPPB) molecules on Ag(111) in the presence of Cl adatoms. The adsorption of the TPyPPB molecules on the clean Ag(111) surface forms an almost defect-free porous SAM stabilized by hydrogen bonds, so-called triangular packing. Such packing can be explored as a host-guest material for atom/molecular confinement. However, in the presence of Cl adatoms, the molecular arrangement changes dramatically. The molecular assembly changes its geometry, forming a non-porous SAM stabilized by H...Cl...H bonds. Such halogen-mediated SAM presents the advantage that the adatom used to stabilize the nanostructure has less influence on the electronic density compared to the typical metal adatoms.

Keywords: On-surface synthesis, STM, Self-assembly monolayer, Nanoporous networks.

Acknowledgments: This work was financially supported by FAPESP (2021/04411-1), FAPESP (2022/12929-3), CNPq, and CAPES (627946/2021-00).

References

1. Fan, Q. et al. *Accounts of Chemical Research* 48, 2484–2494 (2015).
2. Pawlak, R. et al. *Journal of the American Chemical Society* 142, 12568–12573 (2020)
3. Casalini, S. et al. *Chemical Society Reviews* 46, 40–71 (2017)
4. Shi, Z. et al. *Journal of the American Chemical Society* 133, 6150–6153 (2011)

¹ SSD Morton S. Traum Award Finalist

Surface Science

Room 120 - Session SS+AMS+AS+CA+LS-FrM

Advanced Surface Characterization Techniques & Mort Traum Presentation

Moderators: Donna Chen, University of South Carolina, Charles Sykes, Tufts University

8:15am **SS+AMS+AS+CA+LS-FrM-1 Infrared Spectroscopy as a Surface Science Technique**, *Michael Trenary*, University of Illinois - Chicago **INVITED**
Infrared spectroscopy is widely used to probe the vibrational properties of molecules in the gas, liquid, and solid phases. On the other hand, precise information on the structure and chemistry of solid surfaces, and of molecular adsorbates on solid surfaces, is best gained through use of surface science methods. These methods generally entail the use of single crystals, ultrahigh vacuum conditions, and surface sensitive techniques. Reflection absorption infrared spectroscopy (RAIRS) is a surface sensitive technique that can be used in ultrahigh vacuum to study molecular adsorption on well characterized metal single crystal samples. Unlike many other surface science methods, it can also be used under elevated gas pressures. The spectra obtained display features that are quite distinct from those of other phases of matter. For example, in the gas phase, rotational fine structure greatly complicates the appearance of the spectra but is absent in the spectra of adsorbed molecules. In the liquid phase, spectra are broadened by both static and dynamic effects often making it difficult to resolve vibrational peaks due to different chemical species. In polycrystalline molecular solids, molecules are randomly oriented relative to the electric field directions of the infrared radiation, limiting the value of the spectra as a structural probe. In contrast, when molecules adsorb on metal surfaces, they often adopt a definite orientation with respect to the surface normal. This orientation can be deduced through the surface dipole selection rule, which states that only normal modes with a component of the dynamic dipole moment oriented along the surface normal will be allowed. While IR spectroscopy in several forms has long been used to study molecular adsorption on supported transition metal catalysts, the high degree of heterogeneity of the catalyst surfaces leads to very broad peaks, with full width at half maxima (FWHM) of 10-50 cm^{-1} . In contrast, the FWHM of peaks measured with RAIRS on well-ordered metal surfaces can be quite narrow, in some cases even less than 1 cm^{-1} . When a polyatomic molecule exhibits sharp peaks throughout the mid-IR range, the advantages of performing RAIRS with a Fourier transform infrared spectrometer are most pronounced. This talk will cover the speaker's forty years of research using the technique of RAIRS to study molecular adsorbates on metal surfaces.

8:45am **SS+AMS+AS+CA+LS-FrM-3 Modeling Pipeline Surface Chemistry: Reaction of Monochloramine on Iron Surfaces**, *Kathryn Perrine, S. Pandey, O. Agbelusi*, Michigan Technological University

Monochloramine (NH_2Cl), a secondary disinfectant, is utilized to treat pathogens in the municipal water system, producing fewer halogenated disinfection by-products and lasting longer than free chlorine (hypochlorite). Although a weaker oxidant, NH_2Cl has the potential to corrode the surface of pipeline materials resulting in the dissolution of unwanted species. Copper and lead pipelines have been shown to corrode in chloramine solutions, however on iron materials the surface chemistry is unexplored. Complex chemistry occurs on the surface of pipelines at solution/metal interfaces, thus providing catalytic sites for dissociation, decomposition, and degradation. Iron comprises distribution pipelines and also exists as oxides in soils in the natural environment. Redox reactions occur on the surface of iron materials, thus initiating surface corrosion. Here, various active sites on iron are produced and known for high reactivity with nitrogen compounds. Our group employs a surface science approach to uncovering mechanisms at complex interfaces.

In this study, the reaction of monochloramine (NH_2Cl) was investigated on single crystal Fe(111) in ultra-high vacuum at the gas/solid interface using *in situ* infrared reflection absorption spectroscopy and Auger electron spectroscopy. At -160 °C, NH_2Cl molecularly adsorbs to the surface while the annealing leads to the loss of key vibrational modes, suggesting that either molecular desorption or dissociation occurs. These observations are contrasted with our findings at the solution/iron interface, where polarized modulated infrared reflection absorption spectroscopy (PM-IRRAS), ATR-FTIR, XPS, and XRD were used to assess the various regions after corrosion and their film growth. In solution, localized heterogeneous corrosion

products were observed and identified, suggesting different reaction pathways exist in strongly oxidizing solutions. These findings are important for understanding the mechanism of chloramines and water disinfectants on iron interfaces relevant for water quality, material degradation, and other complex environmental processes.

9:00am **SS+AMS+AS+CA+LS-FrM-4 Development of Tip-Enhanced Raman Spectroscopy for Solid-Liquid Interfaces**, *Naihao Chiang*, University of Houston

Tip-enhanced Raman spectroscopy (TERS) combines the spatial resolution of scanning probe microscopy (SPM) with the chemical sensitivity of Raman spectroscopy. TERS with sub-nanometer resolution has been demonstrated under ultrahigh vacuum conditions. We aim to extend this unprecedented chemical mapping capability to interfacial studies under the solution phase. Specifically, we have developed a scanning ion-conductance microscope for TERS (SICM-TERS) capable of interrogating soft samples. In this presentation, the instrumental design will be discussed first. SICM-TERS probe fabrication and evaluation will be followed. Then, a distance-dependent SICM-TERS measurement on two-dimensional MoS_2 sheets will be used to assess the strain created by the SICM probe in close proximity. Our results demonstrate the potential of combining TERS with SICM for obtaining chemical information at interfaces, thus setting the stage for future investigation into soft materials in electrolytic environments.

9:15am **SS+AMS+AS+CA+LS-FrM-5 Ion Based Pump-Probe: Probing the Dynamics Following an Ion Impact**, *Lars Breuer, L. Kalkhoff, A. Meyer, N. Junker, L. Lasnik*, Universität Duisburg-Essen, Germany; *Y. Yao, A. Schleife*, University of Illinois at Urbana Champaign; *K. Sokolowski-Tinten, A. Wucher, M. Schleberger*, Universität Duisburg-Essen, Germany

The study of ion-surface interactions is crucial for understanding material properties and their atomic-level dynamic responses. The transient nature of these interactions, occurring on ultrafast time scales, has so far limited direct experimental observation and has left the field reliant on computer simulations. Existing experimental methods, such as pump-probe techniques, have faced challenges in generating and precisely timing short, monoenergetic ion pulses essential for capturing these ultrafast phenomena.

Our group has pioneered a novel approach that overcomes these limitations by generating the world's shortest monoenergetic ion pulses in the keV regime, with a current duration of approximately 5 ps. These pulses are produced using femtosecond photoionization of a geometrically cooled gas jet, coupled with miniaturization of the ionization section.

In our experiments, we conduct ion-based pump-probe experiments observing the emission of hot electrons post-ion impact, similar to processes studied in two-photon photoemission (2PPE) experiments. Our findings not only demonstrate the feasibility of our approach and provide direct measurements of the ion pulse characteristics but also offer insights into the non-equilibrium dynamics of electronic excitation in solids following an ion impact. We can track the electronic excitation and determine the temporal evolution of a pseudo electron temperature.

This research opens new avenues for understanding the fundamental processes underlying ion-solid interactions, with significant implications for semiconductor manufacturing and materials science. Our work sets a new standard for temporal resolution in the study of ion-induced phenomena and lays the groundwork for future innovations in the field.

9:30am **SS+AMS+AS+CA+LS-FrM-6 How Hot Plasmonic Heating Can Be: Phase Transition and Melting of P25 TiO_2 from Plasmonic Heating of Au Nanoparticles**, *W. Lu, R. Kayastha, B. Birmingham, B. Zechmann, Zhenrong Zhang*, Baylor University

Plasmonic heating has been utilized in many applications including photocatalysis, photothermal therapy, and photocuring. However, how high the temperature can be reached for the surrounding media due to the collective heating of the plasmonic nanoparticles (NPs) and the impact of the heat dissipation on the surrounding media is not clear. Herein we studied the impact of plasmonic heat generated by resonantly excited gold (Au) NPs on P25 TiO_2 nanoparticle film. Under 532 nm continuous laser irradiation at the surface of the Au- TiO_2 , the surface evaporation of Au nanoparticles and phase transition of TiO_2 were observed at moderate laser power. More importantly, as high as the melting point of TiO_2 of 1830°C is confirmed from the molten TiO_2 rutile phase. When Au/ TiO_2 was irradiated with an off-resonance laser at 638 nm, no phase transformation or melting of TiO_2 was observed. The temperature calculation shows that the heating generated by Au nanoparticles is not localized. The collective heating from an ensemble of Au nanoparticles in the irradiated area produces a global

Friday Morning, November 8, 2024

temperature rise that melts TiO_2 . Our results suggest that the photothermal effect could be a major mechanism in the plasmon-assisted photocatalytic reactions. The experimental observation of the high temperature of the supporting media suggests new applications for utilizing plasmonic heating, for example, additive manufacturing.

9:45am **SS+AMS+AS+CA+LS-FrM-7 Kinetics and Dynamics of Recombinative Desorption of Oxygen from Silver and Rhodium Surfaces, Dan Killelea**, Loyola University Chicago

The ability to obtain velocity distributions of molecules desorbing from surfaces with both high temporal precision and angular resolution provide newfound insight into both the kinetics and the dynamics of recombinative desorption and subsurface emergence.

I will discuss our observations of subsurface oxygen emerging from beneath Rh(111) and how the velocity distribution shifts in comparison to the thermally-dominated desorption pathways found for surface-adsorbed oxygen. In addition, it was recently discovered that decomposition of oxygenaceous surface phases on Ag(111) also exhibit pronounced shifts in the energetics of the desorbing oxygen molecules. I will discuss these observations and their potential impacts in oxidation reactions in heterogeneously catalyzed reactions over transition metal surfaces.

10:00am **SS+AMS+AS+CA+LS-FrM-8 Mort Trau Award Announcement**,

10:30am **SS+AMS+AS+CA+LS-FrM-10 Unveiling Surface Mysteries with XPS Lab from Scienta Omicron, Tamara Sloboda**, Scienta Omicron, Sweden; *P. Amann*, Scienta Omicron, Germany; *B. Gerace, F. Henn, A. Yost, X. Zhang*, Scienta Omicron; *M. Lundwall*, Scienta Omicron, Sweden

Surface analysis is paramount for understanding material properties, and Scienta Omicron's XPS Lab system excels in this realm. Featuring a compression unit for superior count rates and sensitivity, it offers unparalleled quantitative XPS enabled by a true counting multi-anode detector inside the Argus CU analyser. This unique detector employs 128 individual counters connected to a striped-anode array. With a linear response extending to the highest count rates and an exceptional dynamic range, it ensures high resolution precise measurements across various sample types.

The versatility of XPS Lab is evident through its scanning, imaging, snapshot, and dynamic measurement modes (see Figure 1), enabling researchers to tailor their experiments to specific needs. The chemical state mapping capability of the XPS Lab provides comprehensive insights into surface chemistry, empowering researchers to unravel complex phenomena.

Illustrating its prowess, case studies span catalysis, energy storage, semiconductor technology, and biomaterials, showcasing its ability to address diverse research challenges. Recent enhancements further strengthen its capabilities, solidifying XPS Lab as the premier choice for XPS analysis.

In summary, Scienta Omicron's XPS Lab system offers unmatched precision, sensitivity, and versatility, driving advancements in surface science and materials research.

10:45am **SS+AMS+AS+CA+LS-FrM-11 Investigation of Stannane (SnH_4) Decomposition and Sticking Coefficient on Varied Metal Surfaces in EUV Lithography Environments, Emily Greene, N. Barlett, D. Qerimi, D. Ruzic**, University of Illinois at Urbana-Champaign

In the context of extreme ultraviolet (EUV) lithography, the evaporation of tin droplets frequently leads to the deposition of tin on various chamber surfaces, including collector mirrors. A prevalent method to remove this tin deposition involves hydrogen plasma etching, which transforms the deposited tin into stannane (SnH_4). This compound, existing in a gaseous state under operational conditions, can be evacuated from the chamber using a vacuum pump. However, stannane is characterized by its instability, tending to decompose and adhere to various surfaces within the chamber.

To systematically study the decomposition behavior of stannane, a specialized experimental chamber has been designed. This chamber integrates a load-lock mechanism for inserting a test tube containing liquid stannane into a loading section, which is isolated from the main vacuum chamber by a valve. Within the main chamber, a quartz crystal microbalance (QCM), regulated by a cartridge heater, measures the mass of stannane deposits. The QCM will be set to temperatures between 30-300 °C. Upon opening the valve, the stannane vaporizes and interacts with the temperature-controlled QCM, facilitating the quantitative

determination of the sticking coefficient as a function of both the surface material and the temperature.

Stannane is synthesized through the reaction of LiAlH_4 , SnCl_4 , $\text{C}_8\text{H}_{18}\text{O}$, and $\text{C}_4\text{H}_{10}\text{O}_2$. The four chemicals are mixed in a 3-neck flask while under vacuum. The reaction produces SnH_4 which flows through three U-tubes traps. The first trap is held at -96 °C to trap precursors, the second two traps are held at -196 °C and trap the stannane. The stannane is increasingly pure the more traps are used.

This investigation aims to understand and quantify the mechanisms of stannane deposition and decomposition, enhancing the maintenance and efficiency of EUV lithographic systems by optimizing the cleaning protocols for tin contamination.

11:00am **SS+AMS+AS+CA+LS-FrM-12 First Principles Methods for Predicting Surface Reaction Mechanisms for Chemical Functionalization of Semiconductor Surfaces, Roberto Longo, S. Sridhar, P. Ventzek**, Tokyo Electron America Inc.,

The density of semiconductor devices continues to increase, accompanied by the subsequent scaling down of the critical dimension (CD) size, which is now on the order of a few nanometers. This results in device structure changes, from two-dimensional (2D) to three-dimensional (3D) structures, because the CD size has reached its limit of reduction. To accomplish this, precise chemical modification of the required surfaces with atomic scale precision is key to obtain the desired geometric control. Precise modification implies being able to leverage knowledge of individual plasma born species and surface interactions. Unfortunately, species specific chemical interaction mechanisms in the context of reactive ions and chemical etching are still poorly understood for the full range of chemical environments at play. Once dissociated in plasma radicals, there might be a wide array of compositions. For similar atomic compositions, variations in the molecular structure of the chemical precursor can also result in significant differences as to the surface modifications and subsequent etching characteristics. The chemical nature of the surface including coverage and chemical activity add significant dimensionality to the problem of controlling plasma surface interactions in general. We divide the problem of elucidating plasma surface interactions into two major categories for practical purposes: hydrofluorocarbon driven for oxide etch and halogen driven for silicon etch. We present here semiconductor surface modeling with general characteristics and investigate the reaction mechanisms undergone by a large variety of hydrofluorocarbon molecular precursors using density-functional theory (DFT), with a focus on reactive halogen adsorption. Given the large parameter space of this problem, we describe computational approaches that efficiently and accurately generate fundamental data. Physical and chemical surface reactions and the corresponding byproducts are identified, obtaining self-limitation thresholds for each specific functionalizing chemistry. Therefore, our computational results provide valuable insights on the complex physical, chemical, and dynamic molecular and ion interactions with functionalized semiconductor surfaces, paving the road for designing tailored strategies with the desired outcome for each specific system.

Bold page numbers indicate presenter

— A —

Adachi, Y.: SS+2D+AMS-WeA-2, 12
 Agbelusi, O.: SS+AMS+AS+CA+LS-FrM-3, 15
 Ahmad, M.: SS+2D+AMS-WeA-1, **11**
 Amann, P.: SS+AMS+AS+CA+LS-FrM-10, 16
 Ariga-Miwa, H.: SS+AMS-MoM-4, 1
 Asakura, K.: SS+AMS-MoM-4, 1
 Asthagiri, A.: SS+AMS-MoA-12, 6; SS+AMS-MoA-3, 4; SS+AMS-MoA-9, 5
 Austin, D.: SS+AMS-MoA-2, **4**
 Auwärter, W.: SS+2D+AMS-WeM-5, **7**
 — B —
 Baber, A.: SS+AMS-MoA-11, 5
 Bae, D.: SS+AMS-MoA-9, 5
 Balajka, J.: SS+2D+AMS-WeA-5, 12; SS+AMS-MoM-12, 2
 Balasubramanian, G.: SS+2D+AMS-WeA-12, 13
 Banerjee, P.: SS+AMS-MoM-5, 1
 Bara, J.: SS+2D+AMS-WeM-17, 8
 Barlett, N.: SS+AMS+AS+CA+LS-FrM-11, 16
 Bergsman, D.: SS+2D+AMS-WeM-13, **8**
 Berriel, N.: SS+AMS-MoM-5, 1
 Birmingham, B.: SS+AMS+AS+CA+LS-FrM-6, 15
 Blackman, K.: SS+AMS-MoM-5, 1
 Blades, W.: SS+2D+AMS-WeA-11, 13
 Bliem, R.: SS+AMS-MoA-1, 4; SS+AMS-MoM-6, **2**
 Boscoboinik, J.: SS+2D+AMS-WeA-1, 11; SS+2D+AMS-WeM-16, **8**
 Breuer, L.: SS+AMS+AS+CA+LS-FrM-5, **15**
 Brohet, M.: SS+2D+AMS-WeA-10, 13
 — C —
 Campbell, C.: SS+AMS-MoM-15, 3
 Campi, G.: SS+2D+AMS-WeA-15, 14
 Campos Jara, S.: SS+2D+AMS-WeA-10, 13
 Carreño, V.: SS+2D+AMS-WeA-15, 14
 Carreño-Díaz, V.: SS+2D+AMS-WeM-3, 7
 Ceccatto, A.: SS+2D+AMS-WeA-15, **14**; SS+2D+AMS-WeM-3, 7
 Cechal, J.: SS+2D+AMS-WeM-4, 7
 Chan, M.: SS+2D+AMS-WeA-14, 14
 Chiang, N.: SS+AMS+AS+CA+LS-FrM-4, **15**
 Chien, T.: SS+2D+AMS-WeA-12, 13
 Christopher, P.: SS+AMS-MoM-3, 1
 Corkery, P.: SS+2D+AMS-WeA-1, 11
 Cramer, L.: SS+AMS-MoM-3, 1
 — D —
 Daniels, A.: SS+2D+AMS-WeM-7, **7**
 de Siervo, A.: SS+2D+AMS-WeA-15, 14; SS+2D+AMS-WeM-3, **7**
 Debenedetti, W.: SS+AMS-MoA-8, 5
 Denecke, R.: AMS2-WeA-12, 11
 Dhas, J.: SS+2D+AMS-WeM-17, 8
 Diebold, U.: SS+2D+AMS-WeA-5, 12; SS+AMS-MoA-1, 4
 Dissanayake, N.: SS+2D+AMS-WeM-8, 8
 Dissanayake, R.: SS+AMS-MoM-7, 2
 Dohnalek, Z.: SS+AMS-MoA-8, 5
 Dorst, A.: SS+AMS-MoM-7, 2
 Dowben, P.: SS+2D+AMS-WeA-6, 12
 Dürr, M.: SS+2D+AMS-WeM-15, **8**
 — E —
 Eder, M.: SS+AMS-MoA-1, 4; SS+AMS-MoM-12, 2
 — F —
 Farber, R.: SS+2D+AMS-WeM-8, **8**
 Ferreira, E.: SS+2D+AMS-WeA-15, 14; SS+2D+AMS-WeM-3, 7
 Forbes, R.: AMS1-WeA-3, **10**
 Franchini, C.: SS+AMS-MoA-1, 4
 Freiburger, E.: SS+2D+AMS-WeA-15, 14
 Fukutani, K.: SS+AMS-MoM-4, 1

— G —

Gao, M.: SS+AMS-MoM-4, 1
 Gerace, B.: SS+AMS+AS+CA+LS-FrM-10, 16
 Gerrits, N.: SS+AMS-MoM-1, 1
 Glaser, T.: SS+2D+AMS-WeM-15, 8
 Greene, E.: SS+AMS+AS+CA+LS-FrM-11, **16**
 Groot, I.: SS+2D+AMS-WeA-10, **13**
 Guisinger, N.: SS+2D+AMS-WeA-14, **14**
 Gupta, A.: SS+AMS-MoM-5, 1
 — H —
 Happel, E.: SS+AMS-MoM-3, 1
 Hasegawa, J.: SS+AMS-MoM-4, 1
 Hazeldine, K.: SS+AMS-MoM-13, 2
 Hedevang, M.: SS+AMS-MoM-13, 2
 Heldebrant, D.: SS+2D+AMS-WeM-17, 8
 Henn, F.: SS+AMS+AS+CA+LS-FrM-10, 16
 Hibbitts, D.: SS+AMS-MoA-6, 5
 Hirushan, H.: SS+2D+AMS-WeM-8, 8
 Hruza, D.: SS+2D+AMS-WeM-4, 7
 Hütner, J.: SS+2D+AMS-WeA-5, **12**; SS+AMS-MoM-12, 2
 — I —
 Islam, A.: SS+AMS-MoA-5, **4**
 — J —
 Jaekel, S.: SS+2D+AMS-WeA-15, 14
 Jakob, Z.: SS+2D+AMS-WeM-4, 7; SS+AMS-MoA-1, 4
 Jalil, A.: SS+AMS-MoM-3, 1
 Jamir, J.: SS+AMS-MoA-12, 6; SS+AMS-MoA-3, 4
 Janulaitis, N.: SS+AMS-MoM-15, **3**
 Jessup, D.: SS+2D+AMS-WeA-11, 13
 Jiang, N.: AMS2-WeA-11, **11**
 Jing, D.: AMS2-WeA-9, 10
 Junker, N.: SS+AMS+AS+CA+LS-FrM-5, 15
 — K —
 Kalkhoff, L.: SS+AMS+AS+CA+LS-FrM-5, 15
 Kasala, P.: SS+AMS-MoA-13, **6**
 Kathmann, S.: AMS2-WeA-13, **11**; AMS2-WeA-9, 10
 Kayastha, R.: SS+AMS+AS+CA+LS-FrM-6, 15
 Killelea, D.: SS+AMS+AS+CA+LS-FrM-7, **16**; SS+AMS-MoM-7, 2
 Kim, L.: SS+2D+AMS-WeA-12, **13**
 Kim, M.: SS+AMS-MoA-12, 6; SS+AMS-MoA-3, 4; SS+AMS-MoA-9, 5
 Kimmel, G.: SS+AMS-MoA-8, 5
 Koert, U.: SS+2D+AMS-WeM-15, 8
 Kraetz, A.: SS+2D+AMS-WeA-1, 11
 Kugler, D.: SS+2D+AMS-WeA-5, 12
 Kühnle, A.: SS+2D+AMS-WeA-5, 12
 — L —
 Lacount, M.: AMS2-WeA-9, 10
 Lang, J.: SS+2D+AMS-WeA-9, 13
 Lasnik, L.: SS+AMS+AS+CA+LS-FrM-5, 15
 Le, D.: SS+AMS-MoA-2, 4; SS+AMS-MoM-14, 3
 Lee, C.: SS+AMS-MoA-6, 5
 Lewis, F.: SS+AMS-MoM-12, **2**
 Lilley, C.: SS+2D+AMS-WeA-14, 14
 Liu, C.: SS+AMS-MoM-4, 1
 Liu, F.: SS+AMS-MoM-14, 3
 Liu, Y.: SS+2D+AMS-WeA-9, 13
 Longo, R.: SS+AMS+AS+CA+LS-FrM-12, **16**
 Lu, B.: SS+AMS-MoM-4, 1
 Lu, W.: SS+AMS+AS+CA+LS-FrM-6, 15
 Lundwall, M.: SS+AMS+AS+CA+LS-FrM-10, 16
 — M —
 Machamer, K.: SS+AMS-MoM-5, 1
 Marquis, E.: AMS1-WeA-5, 10
 McEwen, J.: AMS2-WeA-12, 11
 Meier, M.: SS+AMS-MoA-1, 4
 Meyer, A.: SS+AMS+AS+CA+LS-FrM-5, 15
 Meyer, J.: SS+AMS-MoM-1, 1

Mohrhusen, L.: SS+AMS-MoM-13, 2
 Montemore, M.: SS+AMS-MoM-3, 1
 Mowbray, D.: SS+2D+AMS-WeA-15, 14
 — N —
 Nikolla, E.: AMS2-WeA-12, 11
 Niu, Y.: SS+2D+AMS-WeA-11, 13; SS+AMS-MoA-14, **6**
 Nykpanchuk, D.: SS+2D+AMS-WeA-1, 11
 — O —
 O'Connor, C.: SS+AMS-MoA-8, 5
 Ogaki, T.: SS+2D+AMS-WeA-2, 12
 Ogura, S.: SS+AMS-MoM-4, 1
 Orson, K.: SS+2D+AMS-WeA-11, **13**
 — P —
 Pandey, S.: SS+AMS+AS+CA+LS-FrM-3, 15
 Papp, C.: SS+2D+AMS-WeA-15, 14
 Park, N.: SS+AMS-MoA-9, 5
 Parkinson, G.: SS+AMS-MoA-1, 4; SS+AMS-MoM-12, 2
 Patel, R.: SS+2D+AMS-WeA-1, 11
 Pathan, M.: SS+AMS-MoM-5, 1
 Pavelec, J.: SS+AMS-MoA-1, 4; SS+AMS-MoM-12, 2
 Penland, L.: SS+2D+AMS-WeM-8, 8
 Perrine, K.: SS+AMS+AS+CA+LS-FrM-3, **15**
 Peters, J.: SS+2D+AMS-WeM-15, 8
 Plaisance, C.: SS+AMS-MoA-6, 5
 Planer, J.: SS+2D+AMS-WeM-4, 7
 Pookpanratana, S.: SS+2D+AMS-WeA-3, **12**
 Pope, C.: SS+AMS-MoA-12, **6**; SS+AMS-MoA-3, 4
 Prerna, P.: SS+2D+AMS-WeA-1, 11
 Prochazka, P.: SS+2D+AMS-WeM-4, 7
 Prozorov, T.: AMS2-WeA-9, **10**
 Puntsher, L.: SS+AMS-MoA-1, 4
 — Q —
 Qerimi, D.: SS+AMS+AS+CA+LS-FrM-11, 16
 Qi, J.: AMS1-WeA-5, 10
 Qin, T.: SS+2D+AMS-WeM-1, 7
 — R —
 Rahman, T.: SS+AMS-MoA-2, 4; SS+AMS-MoM-10, 2; SS+AMS-MoM-14, 3
 Ramasubramanian, S.: SS+AMS-MoA-3, 4; SS+AMS-MoA-6, 5
 Rath, D.: SS+AMS-MoM-12, 2
 Ravula, S.: SS+2D+AMS-WeM-17, 8
 Reddy, K.: SS+AMS-MoA-5, 4
 Reddy, R.: SS+AMS-MoA-12, 6
 Reinke, P.: SS+2D+AMS-WeA-11, 13
 Reutt-Robey, J.: SS+AMS-MoA-14, 6
 Rodriguez, J.: SS+AMS-MoA-13, 6; SS+AMS-MoA-5, 4
 Roorda, T.: SS+2D+AMS-WeA-10, 13
 Ruzic, D.: SS+AMS+AS+CA+LS-FrM-11, 16
 — S —
 Sabath, F.: SS+2D+AMS-WeA-5, 12
 Sadowski, J.: SS+2D+AMS-WeA-11, 13
 Sakaguchi, I.: SS+2D+AMS-WeA-2, 12
 Schäfer, T.: SS+AMS-MoM-7, **2**
 Scharf, D.: SS+2D+AMS-WeM-15, 8
 Schleberger, M.: SS+AMS+AS+CA+LS-FrM-5, 15
 Schleife, A.: SS+AMS+AS+CA+LS-FrM-5, 15
 Schmid, M.: SS+2D+AMS-WeA-5, 12; SS+AMS-MoA-1, 4
 Segrest, E.: SS+AMS-MoM-5, 1
 Shahsavari, A.: SS+2D+AMS-WeM-4, 7
 Shang, A.: SS+2D+AMS-WeA-13, 13
 Shang, Z.: SS+2D+AMS-WeA-13, 13
 Sharma, P.: SS+2D+AMS-WeA-12, 13
 Sheng, X.: SS+2D+AMS-WeA-13, **13**
 Sherazi, S.: SS+AMS-MoM-14, **3**
 Shimizu, K.: SS+AMS-MoM-4, 1
 Shin, J.: SS+AMS-MoA-6, 5

Author Index

- Siepmann, J.: SS+2D+AMS-WeA-1, 11
Sloboda, T.: SS+AMS+AS+CA+LS-FrM-10, **16**
Sokolowski-Tinten, K.: SS+AMS+AS+CA+LS-FrM-5, 15
Sombut, P.: SS+AMS-MoA-1, 4
Sridhar, S.: SS+AMS+AS+CA+LS-FrM-12, **16**
Stacchiola, D.: SS+AMS-MoA-7, **5**
Steinrück, H.: SS+2D+AMS-WeA-15, 14
Strange, L.: SS+2D+AMS-WeM-17, 8
Stratton, S.: SS+AMS-MoM-3, 1
Subedi, A.: SS+2D+AMS-WeA-6, **12**
Sudarshan, C.: SS+AMS-MoA-6, 5
Suzuki, T.: SS+2D+AMS-WeA-2, **12**
Sykes, C.: SS+2D+AMS-WeM-7, 7
Sykes, E.: SS+AMS-MoM-3, 1
— **T** —
T. Lee, D.: SS+2D+AMS-WeA-1, 11
Takakusagi, S.: SS+AMS-MoM-4, **1**
Tenney, S.: SS+2D+AMS-WeA-1, 11
Tian, Y.: SS+AMS-MoA-5, 4
Tong, X.: SS+2D+AMS-WeA-1, 11
Trenary, M.: SS+AMS+AS+CA+LS-FrM-1, **15**
Tsapatsis, M.: SS+2D+AMS-WeA-1, 11
Turner, G.: SS+AMS-MoM-5, 1
— **V** —
Vaida, M.: SS+AMS-MoM-5, 1
van den Bosch, F.: SS+AMS-MoM-1, 1
Vang Lauritsen, J.: SS+AMS-MoM-13, 2
Ventzek, P.: SS+AMS+AS+CA+LS-FrM-12, **16**
Verma, K.: AMS2-WeA-9, 10
Visart de Bocarmé, T.: AMS1-WeA-1, **10**
Vovk, E.: SS+2D+AMS-WeA-9, 13
— **W** —
Waleska-Wellenhofer, N.: SS+2D+AMS-WeA-15, 14
Wang, C.: SS+AMS-MoA-1, 4
Wang, D.: SS+2D+AMS-WeA-9, 13
Wang, H.: SS+2D+AMS-WeA-13, 13
Wang, X.: SS+AMS-MoA-8, **5**
Weaver, J.: SS+AMS-MoA-12, 6; SS+AMS-MoA-3, **4**; SS+AMS-MoA-6, 5; SS+AMS-MoA-9, 5
Wen, Y.: AMS2-WeA-9, 10
Whitten, A.: AMS2-WeA-12, **11**
Windl, W.: AMS1-WeA-5, **10**
Wucher, A.: SS+AMS+AS+CA+LS-FrM-5, 15
— **X** —
Xie, S.: SS+AMS-MoM-14, 3
Xu, X.: SS+2D+AMS-WeA-6, 12
— **Y** —
Yang, D.: SS+2D+AMS-WeA-6, 12
Yang, Y.: SS+2D+AMS-WeA-9, **13**
Yao, J.: SS+2D+AMS-WeM-17, **8**
Yao, Y.: SS+AMS+AS+CA+LS-FrM-5, 15
Ye, K.: SS+AMS-MoM-14, 3
Yost, A.: SS+AMS+AS+CA+LS-FrM-10, 16
Yun, J.: SS+AMS-MoA-12, 6; SS+AMS-MoA-3, 4; SS+AMS-MoA-9, **5**
— **Z** —
Zakharov, A.: SS+2D+AMS-WeA-11, 13
Zechmann, B.: SS+AMS+AS+CA+LS-FrM-6, 15
Zhang, X.: SS+2D+AMS-WeA-13, 13; SS+AMS+AS+CA+LS-FrM-10, 16
Zhang, Z.: SS+AMS+AS+CA+LS-FrM-6, **15**
Zhao, K.: SS+AMS-MoM-15, 3
Zhu, J.: SS+2D+AMS-WeM-1, **7**
Zhu, Z.: SS+2D+AMS-WeM-17, 8